Patterns of Pulmonary Structural Remodeling After Experimental Paraquat Toxicity

The Morphogenesis of Intraalveolar Fibrosis

YUH FUKUDA, MD, PhD,
VICTOR J. FERRANS, MD, PhD,
CARL I. SCHOENBERGER, MD,
STEPHEN I. RENNARD, MD, and
RONALD G. CRYSTAL, MD

From the Pathology and Pulmonay Branchés, National Heart, Lung, and Blood Institute, National Institutes of Health, Bethesda, Maryland

For a study of the evolution of interstitial and intraalveolar fibrosis, ultrastructural and immunohistochemical observations were made of the lungs of 16 cynomolgous monkeys given 1 or 2 injections of 10 mg/kg of paraquat and sacrificed 2 days to 8 weeks later. At 2–3 days, alveolar epithelial cells were denuded in many areas, and fibronectin was conspicuous in alveolar spaces. At 1 week, fibroblasts and inflammatory cells were migrating through gaps in the denuded epithelial basement membranes; Type II cells were regenerating in some areas. At 3–4 weeks, alveoli developing intraalveolar fibrosis contained many myofibroblasts, collagen fibrils, and small elastic fibers; fibrotic alveolar walls were lined by metaplastic squamous cells and bronchiolar epithelial cells. Spiraling collagen fibrils were found in interstitium but not in alveolar spaces, which suggests that they were formed from breakdown of collagen. Newly formed intraalveolar collagen was mainly Type I. At 8 weeks, intraalveolar fibrosis had led to extensive remodeling, with new glandlike alveoli lined by Type II cells; alveoli without intraalveolar fibrosis had more normal architecture. Thus, intraalveolar fibrosis in paraquat-treated lung is mediated by intraalveolar migration of interstitial cells, through gaps in the epithelial basement membranes, after epithelial injury. This is followed by connective tissue synthesis on the luminal side of the epithelial basement membrane, by differentiation of interstitial cells into myofibroblasts and smooth-muscle cells, by incorporation of areas of intraalveolar fibrosis into the interstitium, and by coalescence of alveolar walls. Intraalveolar fibrosis is more important than interstitial fibrosis in the structural remodeling that occurs in paraquat-treated lung, because it results in obliteration of alveoli, coalescence of alveolar walls, and loss of functional alveolar–capillary units. (Am J Pathol 1985, 118:452–475)

THE INTERSTITIAL LUNG disorders are characterized by structural remodeling associated with the deposition of fibrous tissue in the lung. Although this fibrosis is classically conceptualized as being interstitial, ie, caused by deposition of fibrous tissue within the alveolar walls, evaluation of open lung biopsies from patients with interstitial disease suggests that intraalveolar fibrosis[1] and coalescence of alveolar walls[2,3] also commonly characterize the structural derangements found in these disorders. Furthermore, the remodeled, fibrotic alveolar walls frequently become lined by increased numbers of Type I alveolar epithelial cells and by cuboidal or squamous metaplastic cells.[2–5] As these disorders progress to "end-stage" or "honeycomb" lung, there is very extensive remodeling of alveolar structures. The sequential steps by which the lung undergoes this remodeling process are not completely understood. To help define the changes that accompany this process, we have used the herbicide paraquat[6–12] to produce both interstitial and intraalveolar fibrosis in cynomolgous monkeys. In this communication we describe the results of sequential examination of the lungs of these animals, employing histologic and transmission electron microscopic techniques as well as immunohistochemical methods for the localization of various connective tissue components.

Accepted for publication October 22, 1984.

Address reprint requests to Dr. Victor J. Ferrans, National Heart, Lung and Blood Institute, National Institutes of Health, Building 10, Room 7N236, Bethesda, MD 20205.

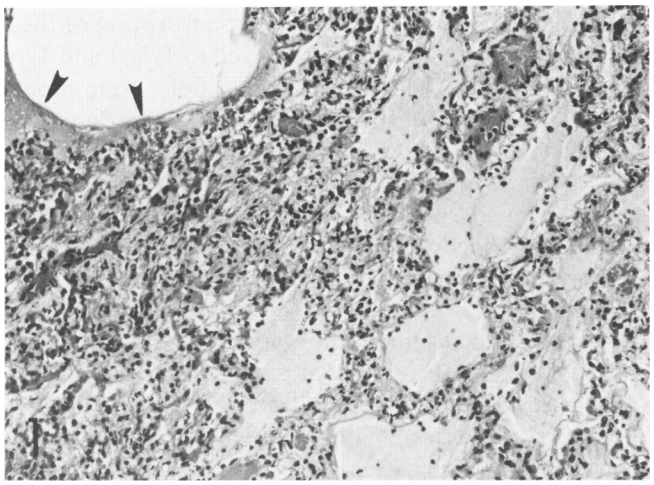

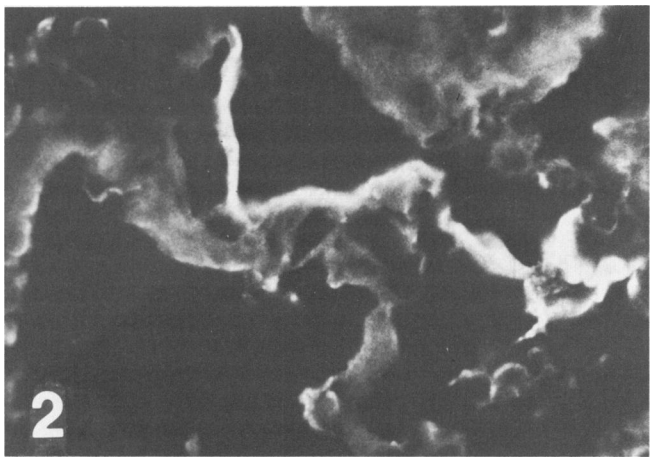

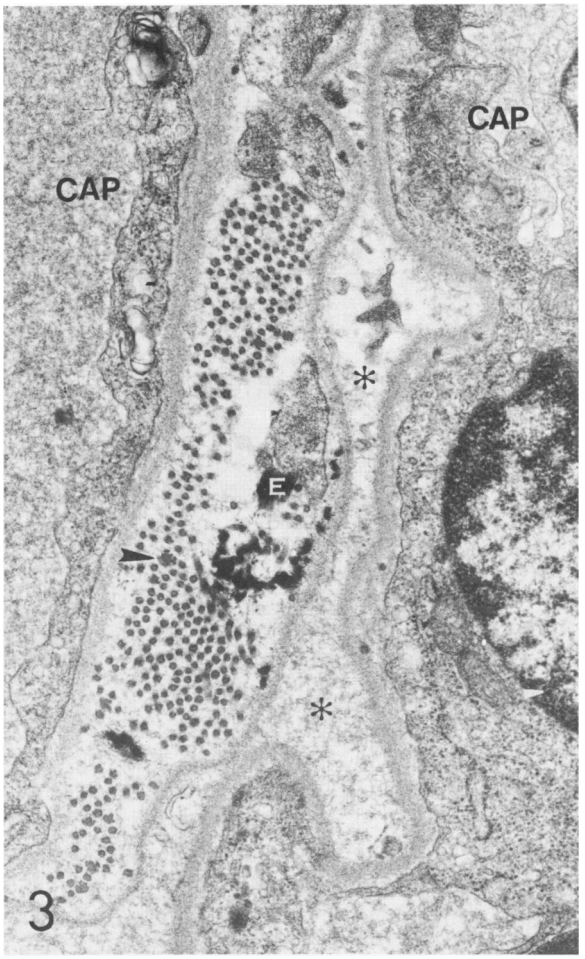

Figure 1—Three days after paraquat administration (Group I). Histologic section showing hyaline membrane formation (*arrowheads*) and marked edema and infiltration with macrophages and neutrophils. (H&E, ×120) **Figure 2**—Group I. Fluorescence micrograph showing localization of fibronectin in alveolar lumens and alveolar walls. (Immunofluorescence, ×300) **Figure 3**—Group I. Parts of two adjacent alveolar walls. Epithelial basement membranes are denuded, and epithelial cell debris and granular materials are found in the intraalveolar space (*asterisks*). The interstitial spaces are edematous and contain capillaries (*CAP*), elastic fibers (*E*), and thin, separated bundles of collagen fibrils, some of which have a spiraling structure (*arrowhead*). (Kajikawa stain, ×25,000)

Materials and Methods

Animal Model

Adult cynomolgous monkeys (*Macaca fascicularis*), weighing approximately 3 kg, were obtained from the National Institutes of Health primate colony. All animals were free of respiratory disease by standard clinical and roentgenographic criteria. The experimental animals were administered paraquat by subcutaneous injection (10 mg/kg, laboratory reagent grade methyl viologen, Sigma, St. Louis, MO, suspended in sterile 0.9% saline) at time 0 and 1 week.

The experimental animals were divided into four groups. Group I (n=3) consisted of the animals which died 2 or 3 days after the first injection of paraquat. The animals in Group II (n=3) were sacrificed 1 week after a single injection of paraquat. The animals in Group III (n=3) received two weekly injections of paraquat and died 3 to 4 weeks after the first injection. The animals in Group IV (n=3) received two weekly injections of paraquat and were sacrificed 8 weeks after the first injection. The control animals (n=4) were given an equal volume of sterile 0.9% saline at time 0 and 1 week and were sacrificed 8 weeks after the first injection of saline.

Histologic Evaluation

The lungs were removed *en bloc*. One of the lobes were excised immediately without inflation and used mainly for immunohistochemical studies (see below). The other lobes were inflated at a pressure of 20 cm of H_2O and fixed by infusion, via the airways, with a

solution of 4% paraformaldehyde–1% glutaraldehyde in phosphate buffer, pH 7.2.[13]

Selected blocks of tissue were embedded in paraffin or in glycolmethacrylate. Histologic sections of paraffin-embedded tissues were stained with hematoxylin and eosin (H&E), Masson's trichrome, and Hart's method for elastic fibers. Histologic sections of glycolmethacrylate-embedded tissues were stained with hematoxylin-eosin, Giemsa, periodic acid–Schiff (PAS), and Gomori's silver impregnation method for reticulin.

Light-Microscopic Immunoperoxidase and Immunofluorescence Methods for Detection of Connective-Tissue Components

Unfixed tissue blocks were frozen in dry ice–acetone and were stored in liquid N_2. Frozen sections were cut at a thickness of 3 μ, immersed in acetone for 5 minutes, and air-dried. These sections were then incubated for 30 minutes at room temperature with rabbit or goat serum (depending on the type of second antibody to be used for each procedure) at a dilution of 1:20 with phosphate-buffered saline (PBS), for blocking nonspecific antibody reactions. The sections were then washed with PBS and were incubated for 30 minutes at room temperature with a suitable dilution of one of the following antibodies: rabbit anti-human elastin antibody, rabbit anti-mouse laminin antibody, goat anti-human fibronectin antibody, goat anti-human Type I collagen antibody, goat anti-human Type III collagen antibody, and sheep anti-human collagen Type IV antibody. Anti-elastin antibody was prepared in rabbits against human aortic α-elastin and was found to be specific for elastin by Ouchterlony testing and by immunohistochemical testing (in which the reactivity of the antibody was completely eliminated by absorption with purified elastin). Antiserum to human fibronectin was prepared in goats with fibronectin purified by affinity chromatography and ion exchange chromatography.[14] The antiserum was monospecific as judged by immunodiffusion with human serum and ELISA against other connective-tissue components.

Type I and III collagen were isolated from human skin following pepsin extraction by salt fractionation.[15] These collagens were then utilized for preparation of antisera in goats. Affinity-purified antibodies were then prepared by adsorption and cross-adsorption of these antisera on CNBr sepharose linked to Type I and Type III collagen.[16] The resulting antibodies were monospecific, as demonstrated by ELISA against a variety of connective tissue components.[16]

Antisera to murine laminin and Type IV collagen were raised in sheep. These sera were demonstrated to be monospecific by ELISA and to cross-react with monkey laminin and Type IV collagen by immunohistochemistry.

After washing three times with PBS, the sections were incubated for 30 minutes at room temperature with either peroxidase-labeled anti-rabbit IgG goat IgG (Cappel Laboratories), peroxidase-labeled anti-goat-IgG rabbit IgG (Sigma Chemical Company), or peroxidase-labeled anti-sheep-IgG rabbit IgG (Cappel Laboratories), at 1:20 dilution and washed three times with PBS. The sections were then reacted[17] with a solution of 3,3'-diaminobenzidine and hydrogen peroxide for 5–8 minutes, washed five times with water, counterstained with methyl green, dehydrated, and mounted. The stained tissue sections were observed by brightfield, polarization, and phase contrast microscopy for evaluation of the structure of the alveoli. For the immunofluorescence method, fluorescein isothiocyanate-labeled antibodies (Cappel Laboratories) were used as second antibodies, and sections were observed with a fluorescence microscope.

Transmission Electron Microscopic Studies

For transmission electron microscopic study, tissues were fixed by perfusion with 4% paraformaldehyde and 1% glutaraldehyde in phosphate buffer, pH 7.2,[13] cut into 1-mm cubes, and washed with several changes of 0.1 M phosphate buffer, pH 7.2 The tissues were then postfixed with 1% OsO_4 in Millonig's phosphate buffer, dehydrated, and embedded in Epon 812. For direct correlation with the ultrastructural observations, 1μ-thick sections of tissues embedded in epoxy resin were stained with alkaline toluidine blue and observed with a light microscope. Ultrathin sections were stained either with uranyl acetate and lead citrate or, for evaluation of elastic fibers, with the tannic acid method of Kajikawa et al[18] and examined with a JEOL 100B electron microscope.

Figure 4—One week after paraquat administration (Group II). Some alveolar spaces are occupied by spindle-shaped fibroblasts, macrophages, and other inflammatory cells. (H&E, × 220) **Figure 5**—Group II. Alveoli are lined by Type II cells and contain macrophages in their lumens. (H&E, × 220) **Figure 6**—Group II. Elastic fibers of alveolar walls are wavy and frayed. (Immunoperoxidase, × 300) **Figure 7**—Group II. An alveolus is lined by Type II cells which have prominent nucleoli and protrude into the alveolar lumens. Two capillaries (*CAP*) are present in the interstitium. (× 6000) **Figure 8**—Group II. Electron micrograph showing spiraling collagen fibrils in the alveolar wall. Note (*upper right*) the highly irregular cross-sectional shapes of these fibrils. (Kajikawa stain, × 55,000) **Figure 9**—Group II. Elastic fibers in the alveolar wall are frayed and consist of irregularly shaped amorphous materials (*asterisks*) and many loosely arranged microfibrils (*arrowheads*), which in some areas are dissociated from the amorphous materials. (Kajikawa stain, × 32,000)

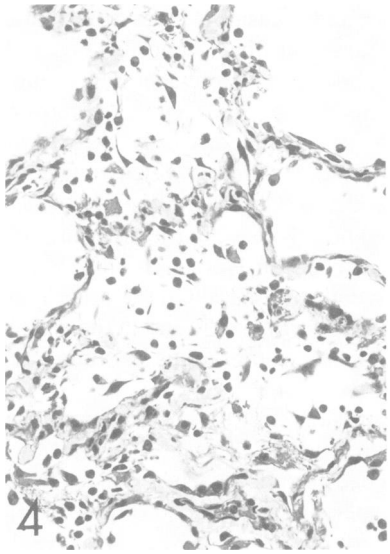
4

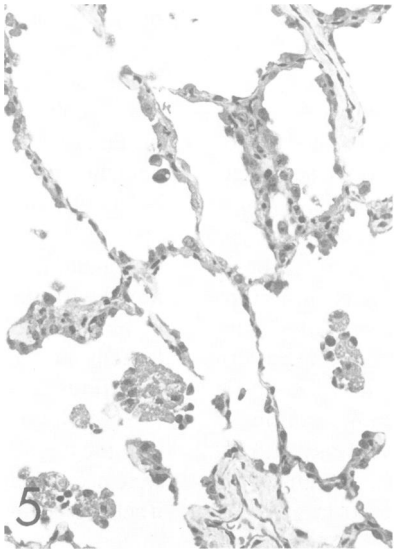
5

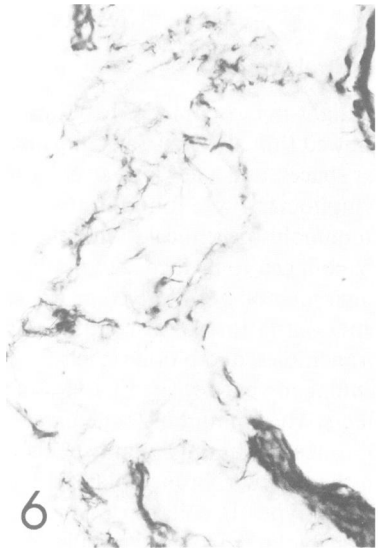
6

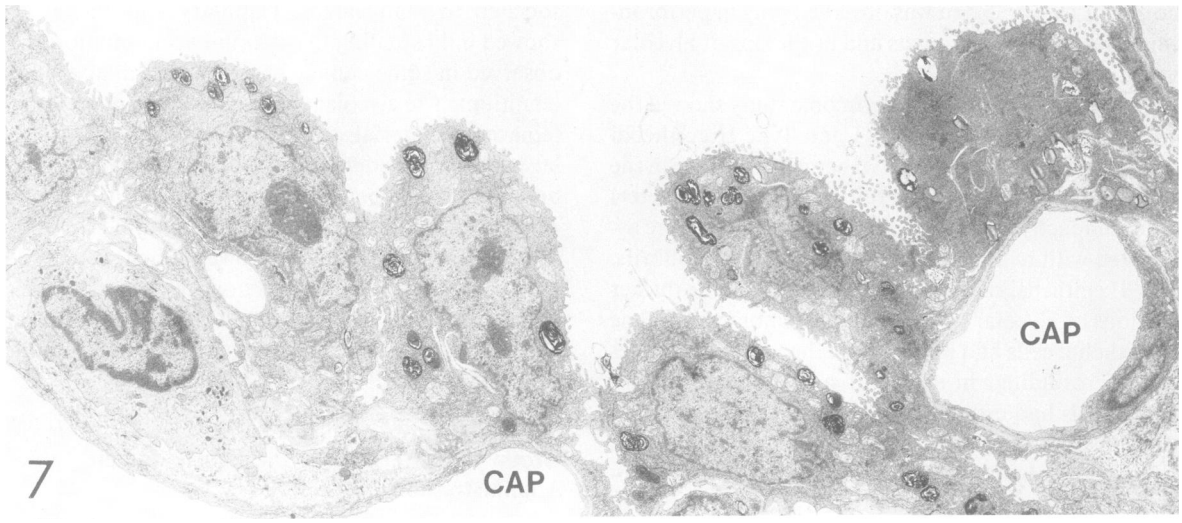
CAP
CAP
7

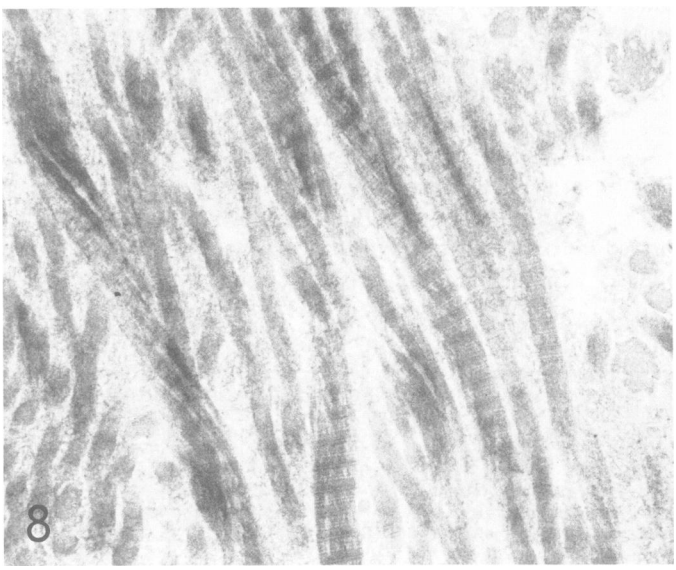
8

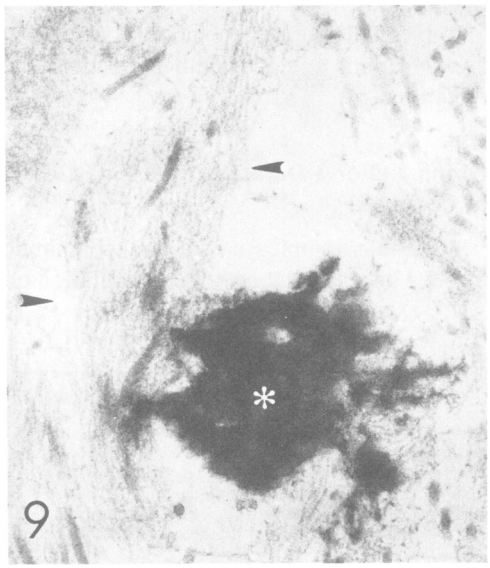
9

Results

Control Animals

Light-microscopic study of lungs of control animals showed thin alveolar walls, normally expanded alveolar spaces, and a few intraalveolar macrophages. A few lymphocytes were found in the peribronchial regions. Immunohistochemical studies showed laminin and Type IV collagen to be localized in the regions of the basement membranes of alveolar walls, vessels, and bronchioles. Elastin was distributed in the walls of alveoli, bronchioles, and blood vessels, with a staining pattern similar to that revealed by Hart's method for elastic fibers. The immunohistochemical staining reaction for fibronectin was only weakly positive and was localized in the alveolar, bronchiolar, and vascular walls. Type I and Type III collagen were distributed in alveolar, bronchiolar, and vascular walls, although a strong reaction for Type I collagen was observed only in peribronchial and perivascular areas and at the tips of alveolar septa.

Transmission electron miscroscopic study showed the normal arrangement of Type I and Type II epithelial cells, capillaries, and interstitial connective tissue in the alveolar walls. The collagen fibrils (60 nm in diameter) were compactly arranged, and the elastic fibers were associated with relatively small amounts of microfibrils. Type II epithelial cells usually were located in the thicker portions of alveolar walls. The cell membranes of Type II epithelial cells had microvilli in the luminal surfaces and microfoldings in the basal surfaces. Type II epithelial cells had discontinuous basement membranes, and interstitial cells had cytoplasmic projections that extended through the areas of discontinuity in the epithelial basement membrane, establishing contact with the basal microfoldings of Type II cells. The capillary and epithelial basement membranes were fused in many areas, forming a single basement membrane (90 nm in thickness).

Group I (2 or 3 Days After the First Dose of Paraquat)

Light-microscopic study of Group I animals showed marked intraalveolar edema, mild dilation or collapse of alveolar lumens, and occasional areas of formation of hyaline membrane and fibrin deposits (Figure 1). Numerous neutrophils and macrophages were found in the alveolar lumens and alveolar septa. In terminal bronchioles, ciliated and mucous cells were focally detached from the epithelial lining, which appeared to be mainly composed of basal cells. Immunohistochemical studies showed no difference in the distribution of elastin, laminin, and collagen Types I, III, and IV, compared with that in control tissues. On the other hand, an abundance of fibronectin was found in the alveolar lumens in the form of membranous or amorphous structures (Figure 2).

Study by transmission electron microscopy showed that most epithelial cells had vacuolar degeneration or were necrotic and had become detached, leaving the epithelial basement membranes denuded (Figure 3). Epithelial and capillary basement membranes were dissociated in many areas. Capillary endothelial cells showed mild swelling. Neutrophil accumulations were observed in some capillary lumens and in alveolar interstitium. The alveolar spaces contained granular proteinaceous materials, cell debris, and fibrin. The alveolar walls were edematous and had thin, separated bundles of collagen fibrils (20–50 nm in diameter). These were associated with a small number of spiraling collagen fibrils, which showed a helical or frayed appearance in longitudinal sections. However, those collagen fibrils which were located in peribronchial and perivascular areas, where they formed thick bundles, were less altered.

Group II (1 Week After the First Paraquat Administration)

One week after the first dose of paraquat, histologic study of the lungs showed focal intraalveolar accumulations of spindle-shaped fibroblasts, macrophages, and other inflammatory cells, associated with an early stage of intraalveolar fibrosis (Figure 4). In other areas there was no intraalveolar fibrosis, but the alveoli had either a conspicuous increase in the numbers of Type II epithelial cells or hyaline membrane formation (Figure 5); both of these changes were found in association with mild thickening of the alveolar walls. Some alveolar

Figure 10—Group II. Early intraalveolar fibrosis. A fibroblast (F_1), which has prominent nucleolus and well-developed rough endoplasmic reticulum, is found in intraalveolar space. Cell debris, fibrin, and other cells, including a macrophage (*M*) and a neutrophil (*N*), also are present in the intraalveolar space. The epithelial basement membrane is denuded; it is labeled (*arrowheads*) to indicate the boundary between the alveolar wall and the alveolar lumen. Cytoplasmic processes attach the intraalveolar fibroblast (F_1) to the luminal side of the denuded epithelial basement membrane. Several capillaries (*CAP*) and other fibroblasts (F_2 and F_3) are present in the alveolar wall. (×5500) **Figure 11**—Group II. High magnification of part of Figure 10, showing attachment of dense cytoplasmic plaque of fibroblast (F_1 in Figure 12) to the luminal surface of the epithelial basement membrane. Fibrin deposits and collagen fibrils (*arrowheads*) are adjacent to the fibroblast in the intraalveolar space and are also present within the alveolar wall (*bottom*). (×24,000) **Figure 12**—High magnification of the area of Figure 11 showing a collagen fibril in intraalveolar space. (×53,000)

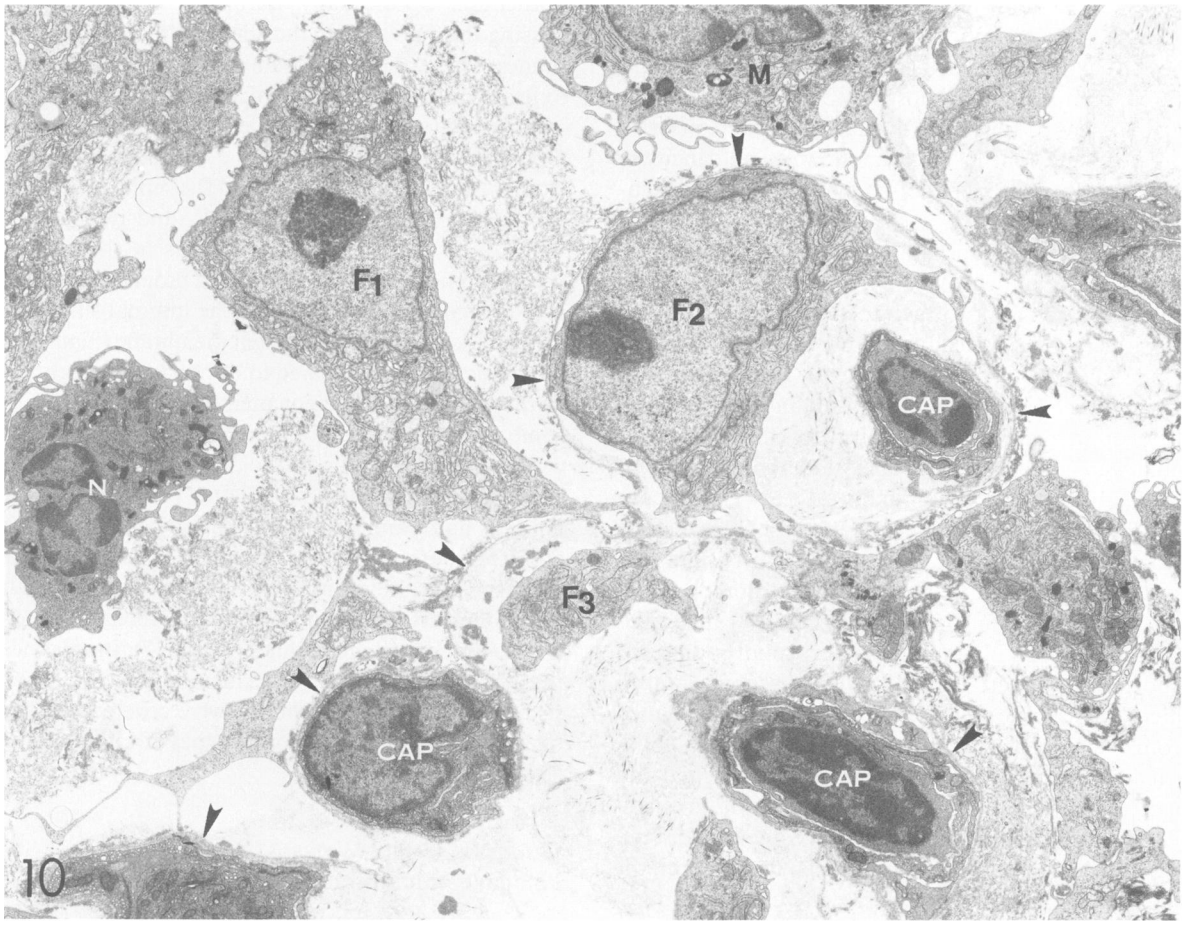
M
F1
F2
CAP
N
F3
CAP
CAP
10

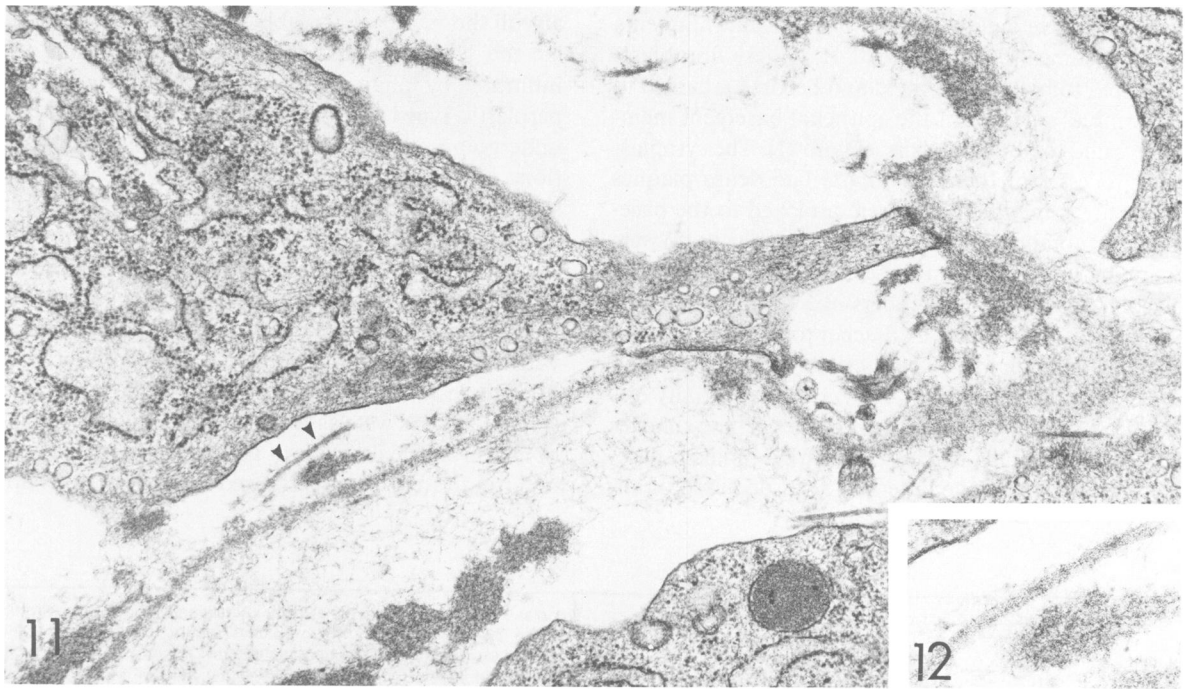
11
12

spaces showed more dilation, in comparison with previous stages. Immunohistochemical study showed that the elastic fibers of alveolar walls were wavy, fuzzy, and frayed, compared with those of control animals (Figure 6). Areas of the alveolar walls which were positive for Type I and Type III collagen showed a mild increase in width. Intraalveolar fibronectin was markedly increased.

Electron-microscopic study confirmed the presence of increased numbers of Type II epithelial cells in areas in which there was no intraalveolar fibrosis. These Type II epithelial cells typically protruded into the alveolar lumens and had prominent nucleoli (Figure 7). These epithelial cells had few basal microfoldings, even though they had increased numbers of microvilli on their luminal and lateral surfaces. Their underlying basement membranes had few discontinuities; there were few contacts between the basal regions of these Type II cells and subjacent interstitial cells. The interstitium was edematous and had many abnormal, spiraling collagen fibrils (80–200 nm in diameter) (Figure 8) and frayed elastic fibers. The latter consisted of poorly outlined amorphous materials and many loosely arranged microfibrils; some microfibril bundles were dissociated from the amorphous materials (Figure 9). The collagen fibrils forming large bundles in peribronchial and perivascular regions and the elastic fibers of large vessels were less altered than those in alveolar interstitium.

In some areas of alveolar epithelial denudation, the intraalveolar spaces contained many elongated fibroblasts, which had large nucleoli, well-developed rough endoplasmic reticulum, and few cytoplasmic filaments and lysosomes (Figures 10 and 11). These fibroblasts appeared to have proliferated and become attached to the luminal surfaces of the epithelial basement membranes and to fibrin deposits (Figure 11). The cytoplasmic processes of these fibroblasts had dense plaques in the areas in which they were attached to the basement membranes. These immature fibroblasts also were found in the interstitium (Figure 10). In these fibrosing alveolar spaces, small numbers of fine collagen fibrils (30 nm in diameter) were adjacent to the proliferating fibroblasts (Figure 12). The alveolar walls surrounding these fibroblasts had thin, wavy, frayed, partially disrupted epithelial basement membranes. These changes were also found, but to a lesser extent, in capillary basement membranes. The latter were not denuded of endothelium. Occasionally, fibroblasts appeared to be passing through gaps in the epithelial basement membranes. These fibroblasts were elongated and appeared to be in the process of becoming attached to the fibrin in the alveolar lumens (Figure 13). In these cells, the Golgi zones were relatively well developed and located closer to the luminal area than to the septal area. Macrophages, neutrophils, eosinophils, and lymphocytes were found together with fibroblasts in the alveolar spaces. Some macrophages that had prominent nucleoli also had come in contact with the luminal surface of the denuded epithelial basement membrane (Figure 14). Lymphocytes also appeared to be passing through gaps in the epithelial basement membrane (Figure 15). In some alveoli where intraluminal fibroblasts were accumulating, regenerating alveolar epithelial cells formed small, glandlike structures (Figure 16). These epithelial cells had prominent rough endoplasmic reticulum and free ribosomes and a few lamellar bodies. The epithelial cells proliferating on the luminal surfaces of the fibrin deposits lining and damaged alveolar walls did not have basement membranes (Figure 17). In areas near the alveolar ducts, the hyaline membranes, which consisted of cell debris and fibrin, were covered by fibroblasts, macrophages, and other types of inflammatory cells (Figure 18).

Group III (3 to 4 Weeks After the First Paraquat Administration)

Three to 4 weeks after the first dose of paraquat, the alveoli showed focal, variably sized areas of intraalveolar and septal fibrosis. Thickened alveolar walls were infiltrated by inflammatory cells and were lined by hyperplastic Type II epithelial cells, cuboidal cells, or cells undergoing squamous metaplasia. Detailed observations on the squamous metaplasia will be reported separately. The animals that had severe intraalveolar fibrosis showed less Type II epithelial-cell hyperplasia and much more bronchiolar epithelial hyperplasia and more squamous-cell metaplasia. This squamous-cell metaplasia was conspicuous in alveolar ducts associated with severely fibrotic, obliterated alveoli (Figure 19). Fibrotic lesions were mainly intraalveolar in location (Figure 20) and were associated with apparent collapse of alveoli and coalescence of alveolar walls. Alveoli with no intraalveolar fibrosis showed emphysematous dila-

Figure 13—Group II. Fibroblastic migration into an alveolar luminal space. A fibroblast (*F*) is passing from the alveolar interstitium (*bottom*) to the alveolar lumen (*top*) through a gap (*arrowheads*) in the epithelial basement membrane. The Golgi zone of this cell is well developed and is located closer to the luminal area. Fibrin deposits are present in the alveolar lumen. The epithelial and capillary (*CAP*) basement membranes are frayed in some areas. (×6700) **Figure 14**—Group II. An intraalveolar macrophage is in close contact with the luminal surface (*arrowheads*) of a denuded alveolar epithelial basement membrane. (×7500) **Figure 15**—Group II. A lymphocyte is passing from the alveolar wall (*bottom*) to the alveolar lumen (*top*) through a gap (*small arrowheads*) in the epithelial basement membrane (*large arrowheads*), which is frayed, thin, and partially disrupted. (×9200)

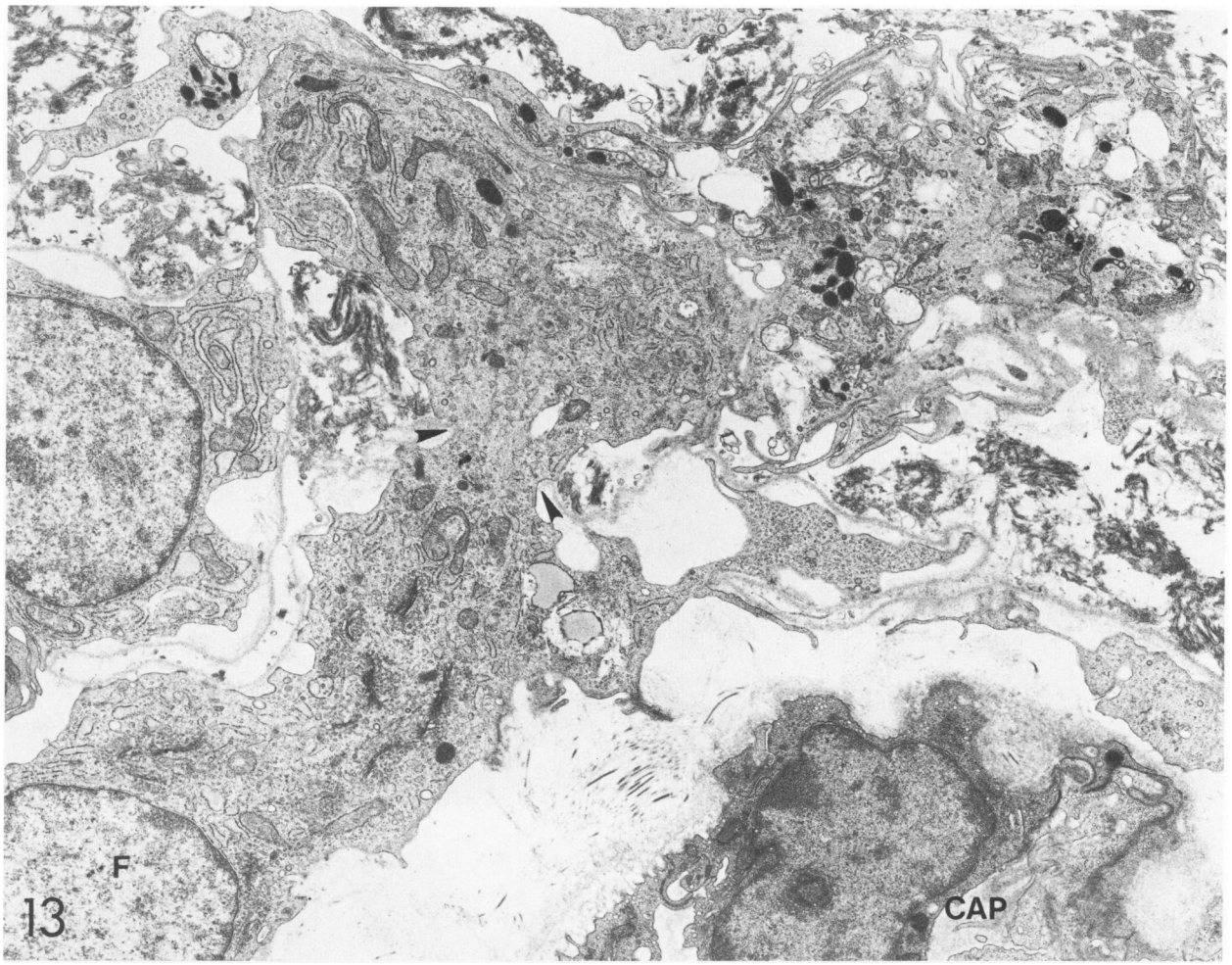

13

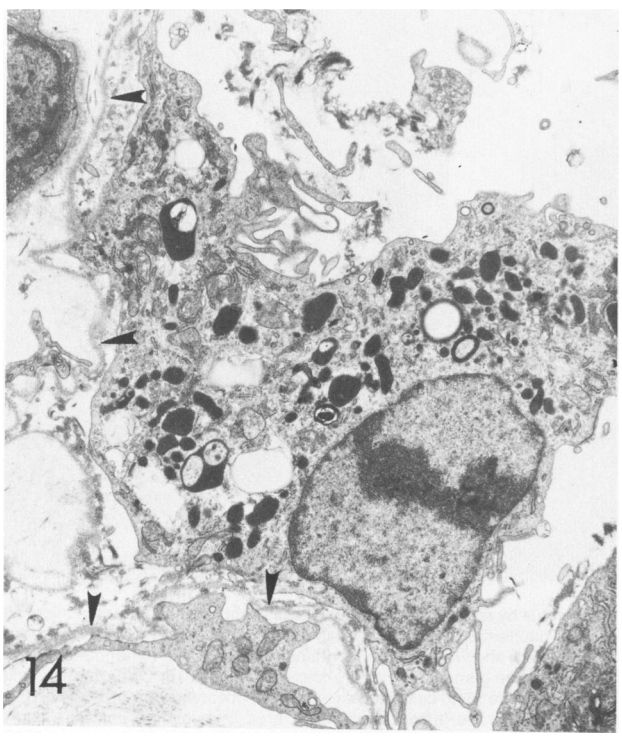
14

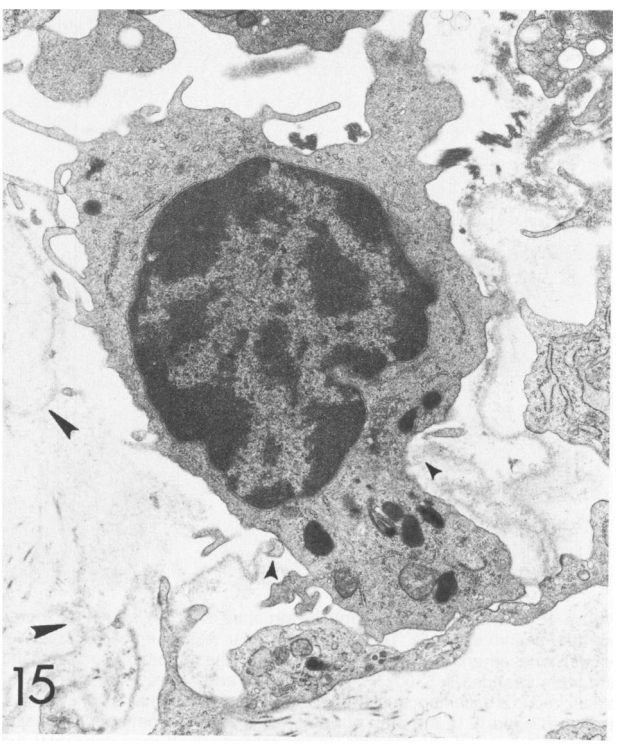
15

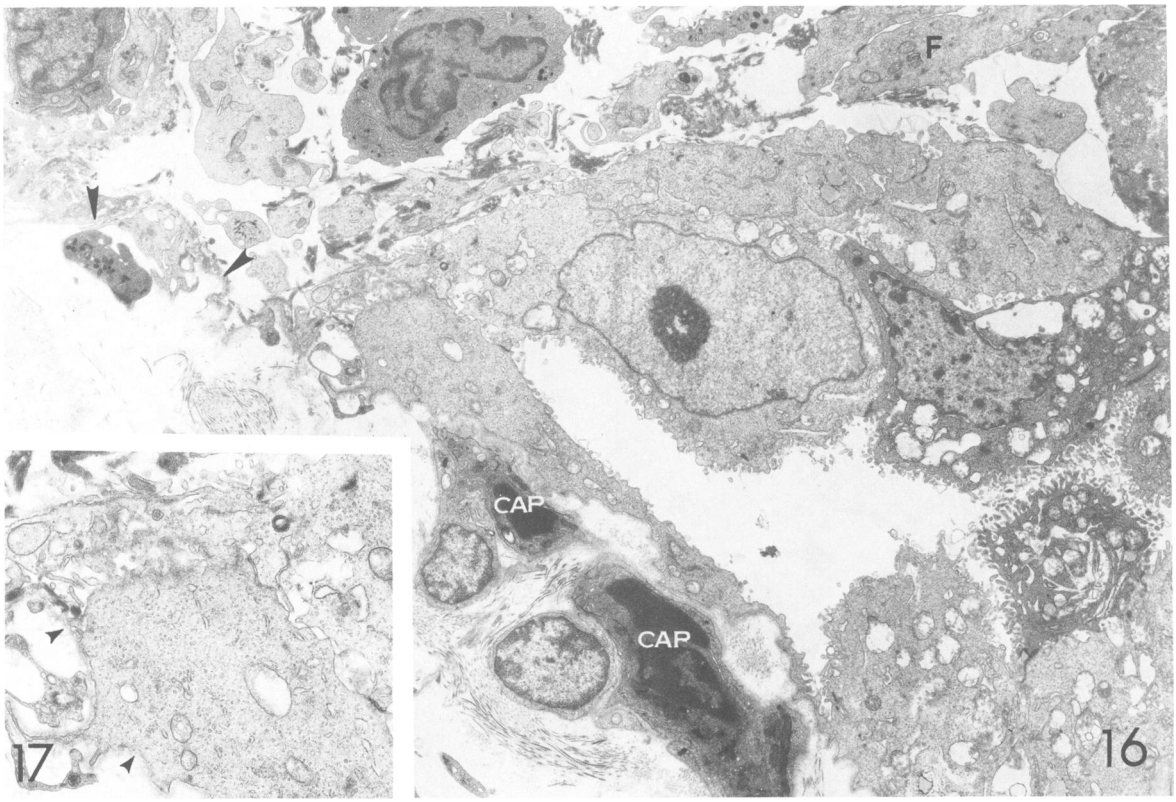

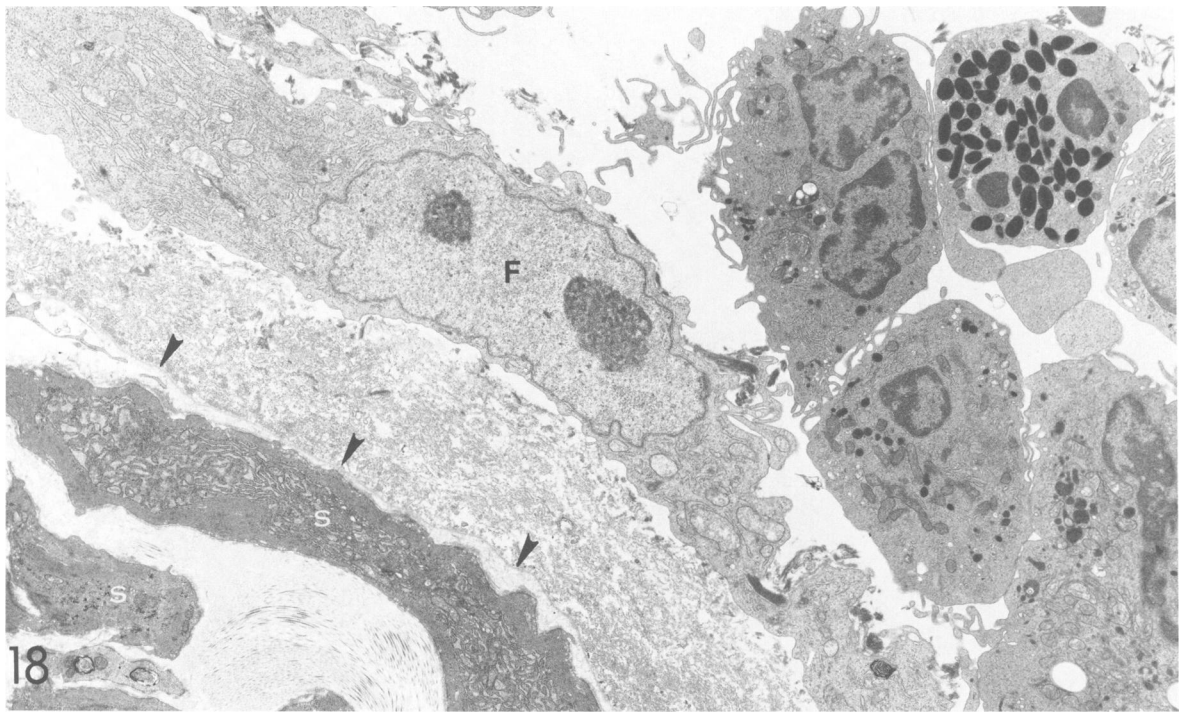

Figure 16—Group II. A small glandlike structure is formed within the lumen of an alveolus by regenerating epithelial cells which have numerous microvilli on their luminal surfaces. The original alveolar wall, seen at the *lower left*, contains capillaries (*CAP*) and collagen fibrils and has a partially denuded epithelial basement membrane (*arrowheads*). The remaining portion of the alveolar lumen, shown at the *top*, contains fibroblasts (*F*), inflammatory cells, and fibrin strands. (× 5300) **Figure 17**—Parts of two regenerating epithelial cells in the glandlike structure shown in Figure 16. One of these cells is attached to a basement membrane (*arrowheads*); the other is not attached on its basal surface. Both cells contain many free ribosomes. (× 11,000) **Figure 18**—Group II. In the area of an alveolar duct, the denuded epithelial basement membrane (*arrowheads*) is covered by hyaline membrane and a fibroblast (*F*); smooth-muscle cells (*S*) and collagen fibrils are subjacent to the basement membrane. Many inflammatory cells are found in the lumen. (× 6600)

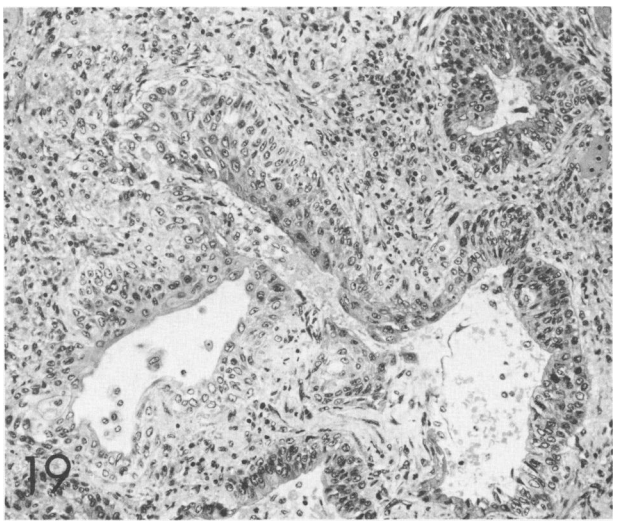

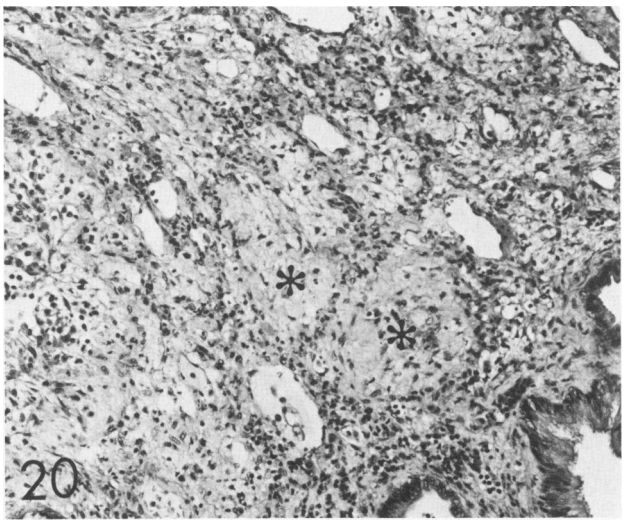

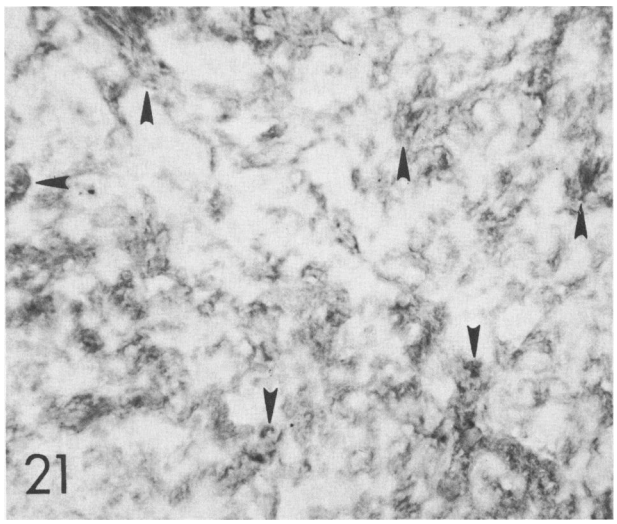

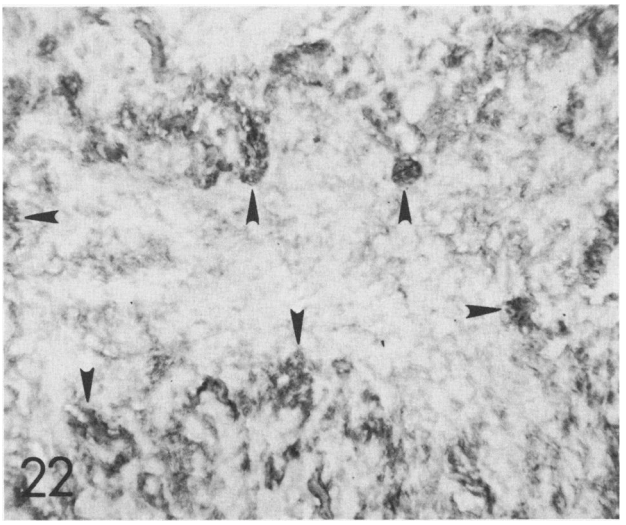

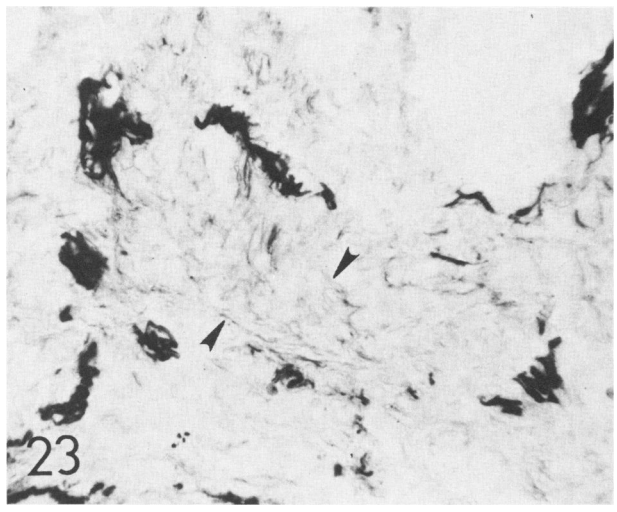

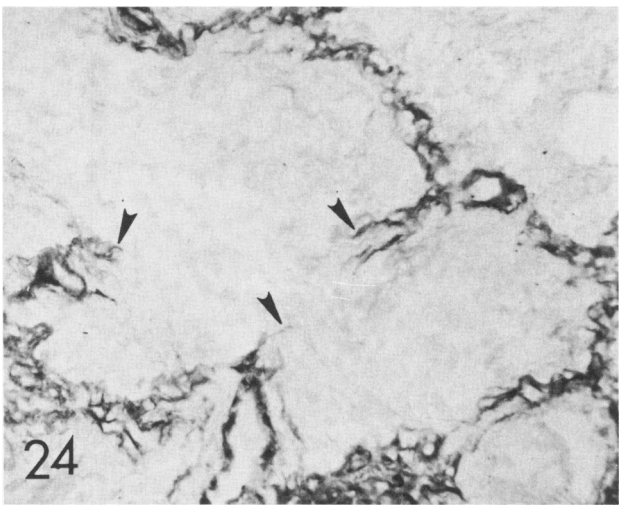

Figure 19—Three to 4 weeks after paraquat administration (Group III). Prominent squamous metaplasia is associated with fibrotic alveoli. (H&E, ×120) **Figure 20**—Group III. Intraalveolar fibrosis (*asterisks*) is prominent at this stage. (H&E, ×120) **Figure 21**—Group III. Type I collagen is demonstrated in areas of intraalveolar fibrosis. The tips of the original alveolar septa (*arrowheads*) appear to have thicker fibers. (Immunoperoxidase, ×220) **Figure 22**—Group III. Type III collagen in areas of intraalveolar fibrosis is much less prominent, compared with the Type I collagen shown in Figure 21. The tips of the original alveolar septa are indicated by *arrowheads*. (Immunoperoxidase, ×220) **Figure 23**—Group III. Fine elastic fibers (*arrowheads*) are detected by the immunoperoxidase method in area of intraalveolar fibrosis. (×220) **Figure 24**—Group III. Reaction for laminin shows staining of epithelial and endothelial basement membranes. Areas of discontinuity (*arrowheads*) probably represent damaged epithelial basement membranes. (Immunoperoxidase, ×220)

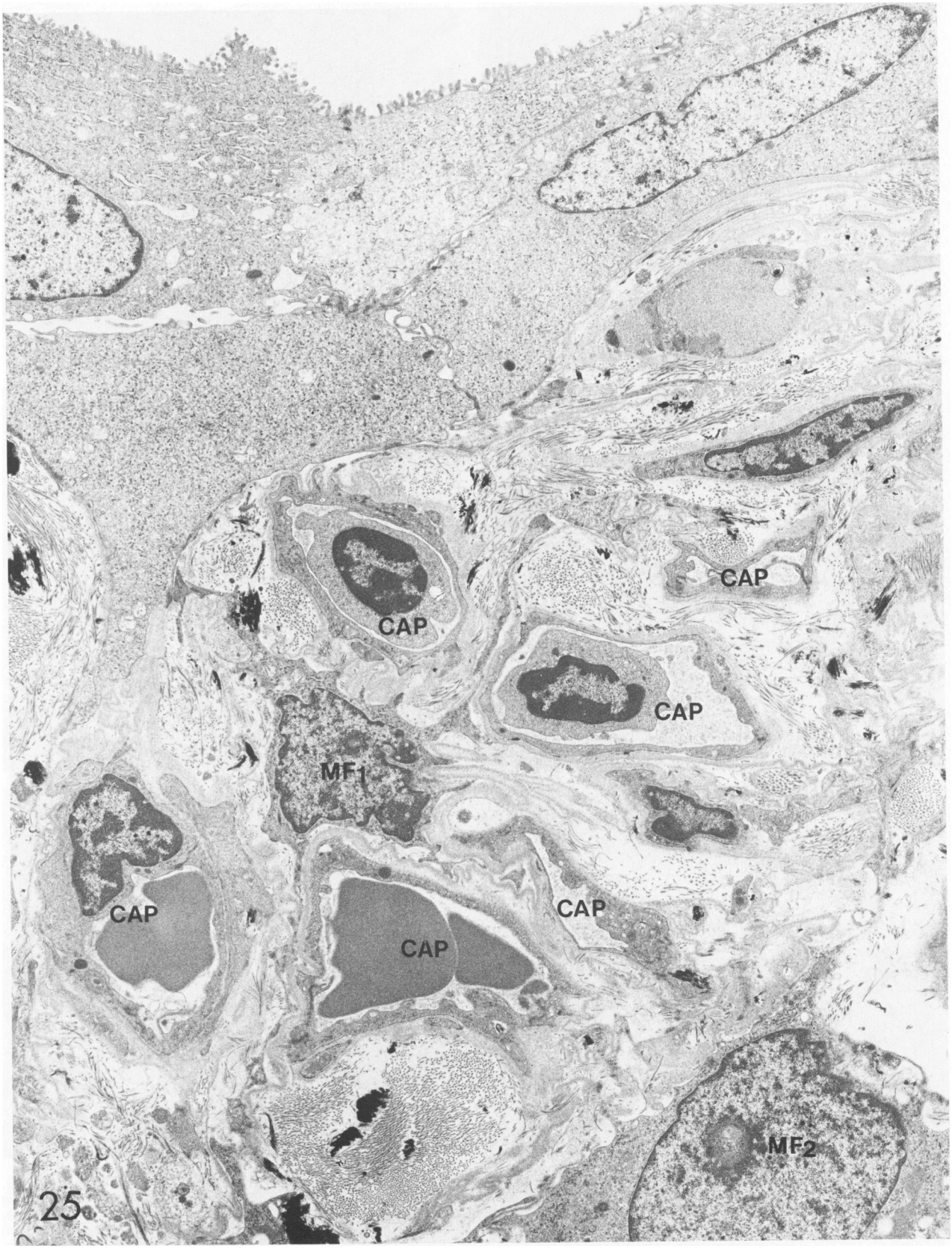
CAP
CAP
CAP
CAP
MF1
CAP
CAP
CAP
MF2
25

tation. Histochemical observations on elastic fibers in these areas will be reported separately.

Immunohistochemical study showed that the intraalveolar fibrotic areas were stained much more intensely by the anti-Type I than by the anti-Type III collagen antibody (Figures 21 and 22). The staining pattern of alveolar walls and areas of intraalveolar fibrosis for fibronectin was similar to that obtained for Type I collagen. Alveolar exudates in some areas of intraalveolar fibrosis were stained strongly for fibronectin. In some areas of intraalveolar fibrosis, staining with antielastin antibody revealed fine fibers (Figure 23), although such fibers were not demonstrable with the use of Hart's method for elastic fibers. Type IV collagen and laminin (Figure 24) showed a discontinuous pattern of staining of the epithelial basement membranes in regions of intraalveolar fibrosis. In basement membranes of other regions, the patterns of staining for Type IV collagen and laminin were similar to those observed in previous stages.

Electron-microscopic study showed that the alveolar walls in many areas were covered by Type II epithelial cells. In areas of severe intraalveolar fibrosis and in collapsed alveoli without alveolar epithelial regeneration, there was conspicuous metaplasia of cuboidal or single-layered or stratified squamous epithelial cells (Figure 25). These epithelial cells sometimes did not cover completely the original epithelial basement membrane, but they covered many of the discontinuities in the epithelial basement membranes and sometimes also the intraluminal mesenchymal cells. Thus, these cells provided a new epithelial lining for the remodeled structures. The original alveolar spaces of the collapsed and coalescent alveoli contained a few myofibroblasts and small amounts of collagen fibrils and elastic fibers. Wavy, discontinuous epithelial basement membranes were common in these lesions of collapsed alveoli and intraalveolar fibrosis.

Many of the cells in the areas of intraalveolar fibrosis were myofibroblasts.[19] These cells had many actin-like filaments and peripherally located dense bodies in their cytoplasm, but had no basement membranes (Figures 25 and 26). Some smooth-muscle cells were also found; they had many dense bodies in their cytoplasm and were surrounded by discontinuous basement membranes (Figure 27). These myofibroblasts and smooth-muscle cells in areas of intraalveolar fibrosis had cytoplasmic processes associated with dense plaques which were attached to the luminal surfaces of the epithelial basement membranes.

The collagen fibrils in intraalveolar spaces measured 60 nm in diameter and had a tendency to form bundles. Proteoglycan granules were conspicuous between loosely arranged collagen fibrils. Small elastic fibers, which had a high proportion of microfibrils, were found in association with collagen fibrils in intraalveolar fibrotic areas (Figure 28). Spiraling collagen fibrils were conspicuous in alveolar interstitium but were not found in areas of intraalveolar fibrosis (Figures 29 and 30). Some macrophages, mast cells, plasma cells, and lymphocytes were associated with intraalveolar accumulations of myofibroblasts. In some areas of intraalveolar fibrosis, large fibroblastlike cells, which appeared to be phagocytosing collagen fibrils, also were attached to the luminal side of the epithelial basement membrane (Figures 31 and 32).

Group IV (8 Weeks After the First Paraquat Administration)

Evidence of a recovery process was found in 8 weeks after the first injection of paraquat. Focal and patchy fibrotic lesions were found within alveolar spaces, in association with mild bronchiolarization of epithelium of alveoli and mild lymphoid cell infiltration, especially in subpleural regions (Figure 33). Squamous metaplasia had regressed. Elastic fiber staining confirmed that the areas of fibrosis consisted of obliterated alveoli with intraalveolar fibrosis and alveolar collapse and coalescence (Figure 34). Glandlike structures lined by cuboidal epithelium were found in these areas. Alveoli with minimal fibrotic changes showed mild to moderate dilatation and still had mildly increased numbers of macrophages in their lumens.

Immunohistochemical study showed that Type I and Type III collagen were similarly distributed. The pattern of distribution of both collagens in the less fibrotic alveolar walls was similar to that seen in control animals. In the areas of fibrosis, including those of intraalveolar fibrosis, Type I and Type III collagen showed similar diffuse distribution patterns. Laminin and Type IV collagen were detected in the basement membranes of the alveoli, bronchioles, and vessels. Stains for laminin (Figure 35) and Type IV collagen showed that the

Figure 25—Group III. A view of a collapsed alveolus, which contains a stellate-shaped myofibroblast (MF_1) in its obliterated lumen. This lumen is demarcated by remnants of denuded epithelial basement membrane. Several capillaries (*CAP*) associated with collagen fibrils and elastic fibers are clustered around this collapsed alveolus. At the *top*, a layer of epithelial cells undergoing squamous metaplasia has lined the lumen of a uncollapsed area of an alveolus. Note the close apposition of a cytoplasmic process of the myofibroblast (MF_1) and the basal portion of an epithelial cell. At *bottom right*, another myofibroblast (MF_2) is shown. This cell is also located within the alveolar lumen (note the remnants of epithelial basement membrane separating the cell from adjacent capillaries). This lumen contains collagen fibrils and therefore is a site of intraalveolar fibrosis. (Kajikawa stain, ×8000)

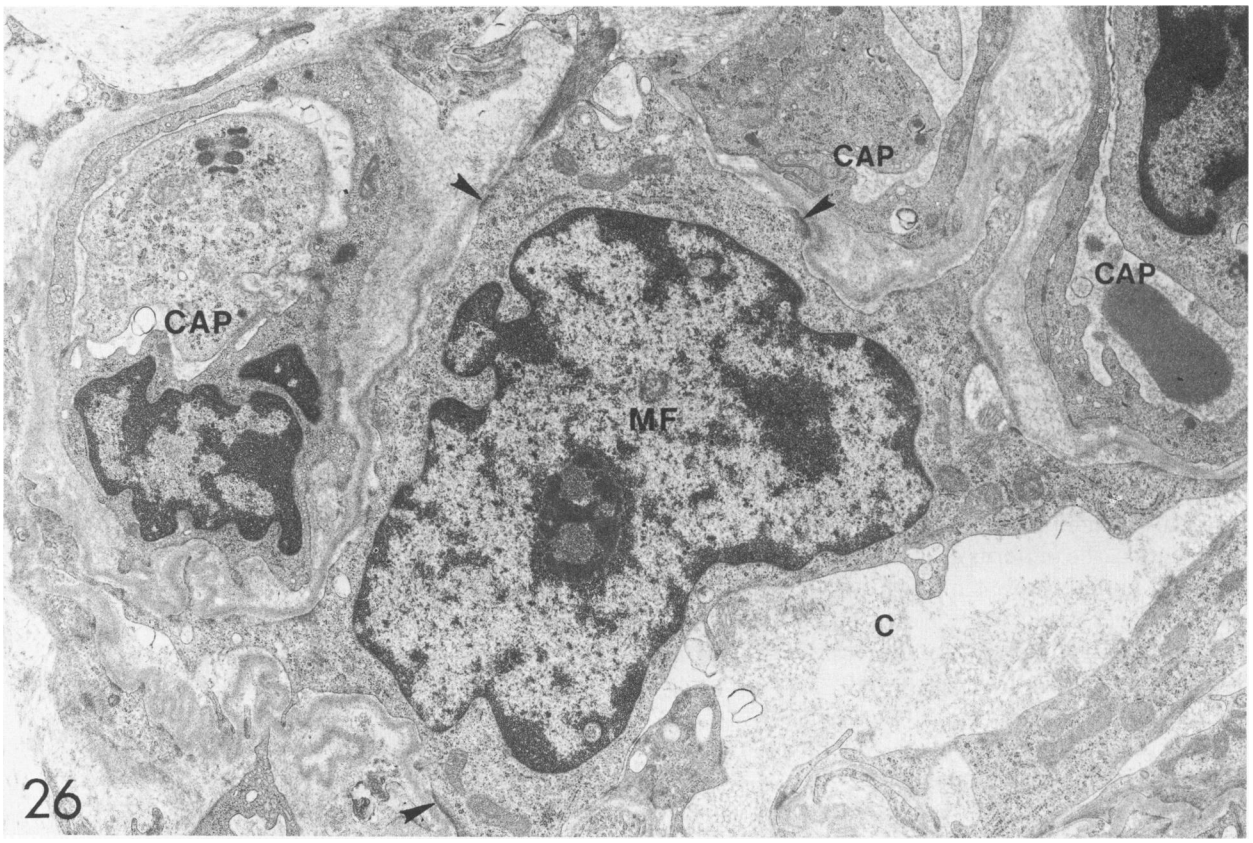
CAP
CAP
CAP
MF
C
26

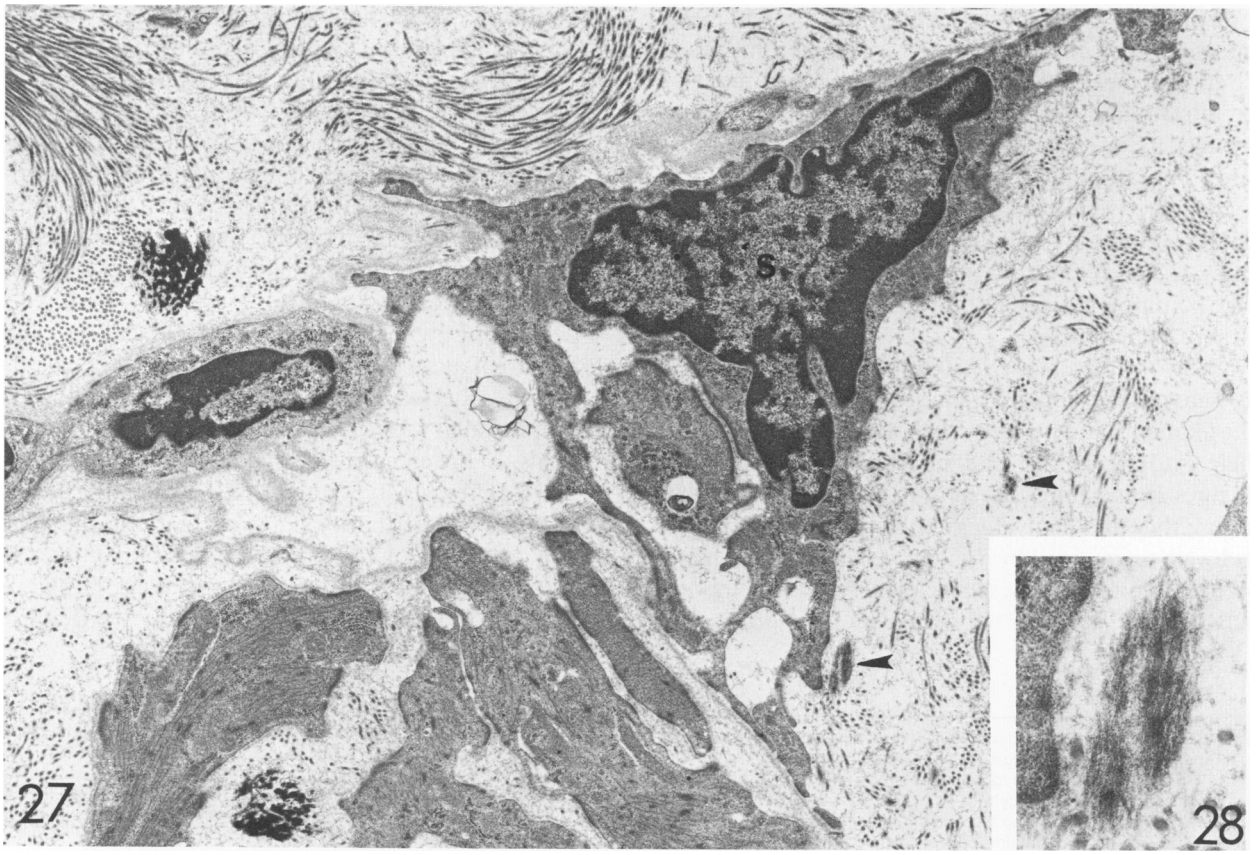
S
27
28

original alveolar walls were embedded in the fibrotic lesions; this staining also outlined the capillary and epithelial basement membrane and showed areas of discontinuity in the latter. In fibrotic regions, elastic fibers in the original areas of the alveolar walls were thinner and discontinuous, compared with those in control animals. Intraalveolar spaces had more developed elastic fibers than in previous stages. Elastin was increased in the tips of alveolar septa in association with hyperplasia of smooth-muscle cells in these septa. Fibronectin was detected in the alveolar walls and in fibrotic lesions, but the reaction was less intense than in previous stages.

Electron-microscopic study showed that the less fibrotic alveolar walls had only a mild increase in the numbers of Type II epithelial cells. These cells extended more deeply than normal into the alveolar interstitium. They had many microfoldings in their basal surfaces, wide gaps in their basement membranes, and many cytoplasmic contacts with interstitial cells. Areas of separation of epithelial and endothelial basement membranes were found in association with increased numbers of collagen fibrils (Figure 36). Spiraling collagen fibrils were conspicuous in the interstitium of alveolar walls (Figure 37). In this stage, elastic fibers were not frayed in the less fibrotic alveolar walls, but some of the amorphous components of the elastic fibers were associated with small, electron-dense, lamellar, nodular masses (Figure 38). Energy dispersive X-ray microanalysis revealed the presence of calcium in these nodules. The fibrotic lesions involved interstitial and intraalveolar regions, although in some areas it was difficult to determine whether these lesions were intraalveolar or not, because of the partial absence of epithelial basement membranes. The numbers of Type II alveolar epithelial cells were increased to a greater extent in these fibrotic regions than in less fibrotic alveolar walls. In these fibrotic areas, many Type II epithelial cells protruded less into the alveolar lumens, although they had discontinuous basement membranes and close contact with the interstitial cells. Within the fibrotic regions, alveolar epithelial cells occasionally formed glandlike structures (Figure 39). The epithelial cells which were attached to the original epithelial basement membrane in these areas were mainly Type I cells; those in intraalveolar fibrotic lesions were Type II cells. Many denuded, wavy, thin, and disrupted epithelial basement membranes were embedded in connective tissue in fibrotic lesions (Figure 40). These lesions corresponded to collapsed and coalescent alveoli. In areas of intraalveolar fibrosis, more elongated myofibroblasts were found than in previous stages. Also present in these areas were macrophages having numerous phagosomes, bundles of collagen fibrils measuring 60 nm in diameter, and small elastic fibers. In fibrotic regions, spiraling collagen fibrils were found exclusively in areas that corresponded to the original alveolar interstitium, and not in areas of intraalveolar fibrosis. Occasionally, frayed elastic fibers were found in areas corresponding to the original alveolar interstitium in fibrotic regions.

Discussion

The observations in the present study extend and confirm previous morphologic findings on the lungs of monkeys with paraquat toxicity.[20,21] These observations are similar to those made in other species, including mouse,[22] guinea pig,[21] rat,[6,9,10,23] rabbit,[24] and dog.[25] They are also consistent with the findings in humans with paraquat-induced pulmonary fibrosis.[7,8,11,12,26,27] Both interstitial and intraalveolar fibrosis have been described in humans and in experimental animals with paraquat toxicity. As discussed in detail below, the present study provides detailed documentation of the series of ultrastructural changes that lead to these two types of fibrosis and to remodeling of lung structures in paraquat toxicity. Analysis of these changes demonstrates that intraalveolar fibrosis is extremely important in mediating the process of pulmonary remodeling.

The pulmonary lesions following paraquat intoxication evolve through two stages: a phase of injury and a proliferative phase.[20] Early events after administration of paraquat, corresponding to the phase of injury, consisted of 1) damage to alveolar epithelial cells resulting in denudation of epithelial basement membranes; 2) alveolitis, manifested by exudation of inflammatory cells (especially macrophages and neutrophils), fibrin, and fibronectin into the alveolar spaces; and 3) alterations in the structure of collagen fibrils, elastic fibers, and epithelial basement membranes. The structural changes in extracellular elements of connective tissue were more severe at 1–4 weeks after paraquat administration, at which time proliferative fibroblastic changes

Figure 26—Group III. A myofibroblast (*MF*) in intraalveolar space has peripherally located cytoplasmic dense plaques (*arrowheads*), is associated with collagen fibrils (*C*), and is separated from adjacent capillaries (*CAP*) by wavy epithelial basement membranes. (× 13,000) **Figure 27**—Group III. Smooth-muscle cells (*S*) are present in an intraalveolar space and are separated from other smooth-muscle cells, which are located within the alveolar wall, by wavy basement membrane. Note the fine elastic fibers (*arrowheads*) and collagen fibrils in the intraaveolar space and larger elastic fibers in the alveolar wall. (Kajikawa stain, × 13,000) **Figure 28**—Intraalveolar elastic fibers shown in Figure 27 are fine and consist of small amorphous components and many microfibrils. (Kajikawa stain, × 35,000)

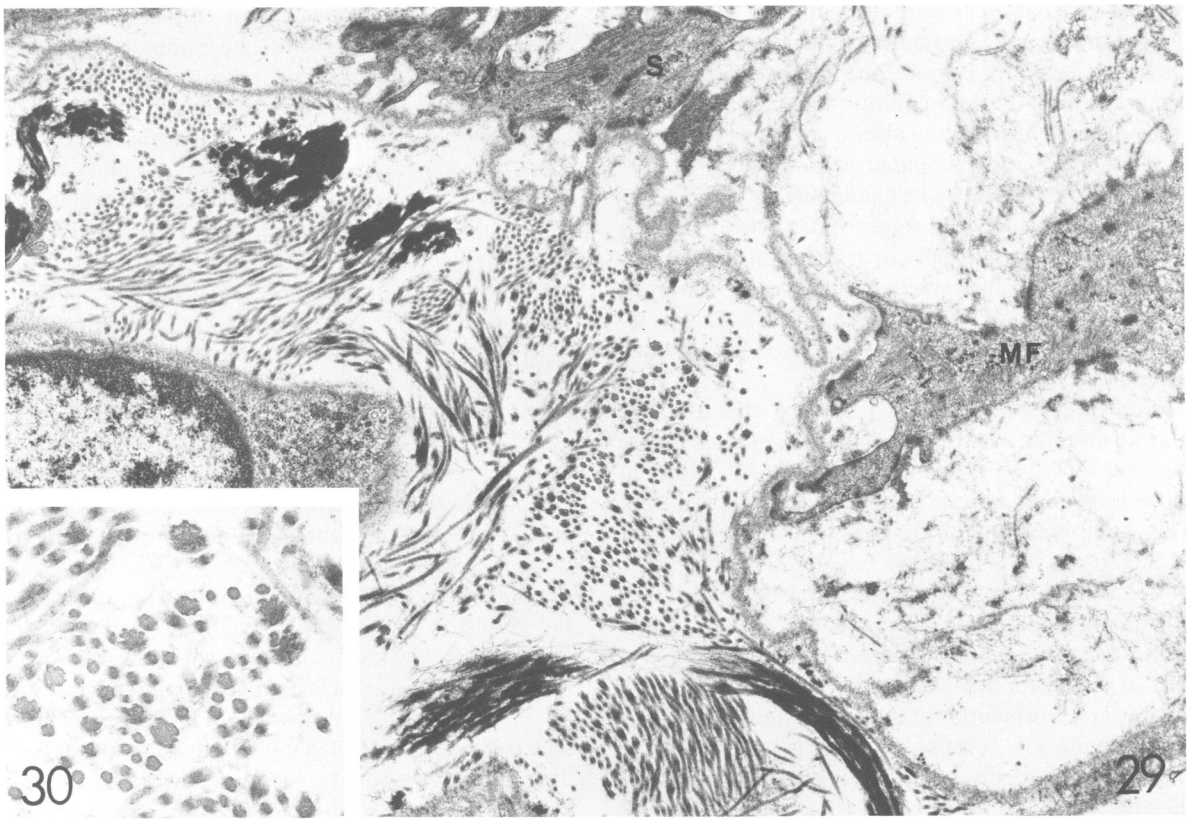
S
MF
29

30

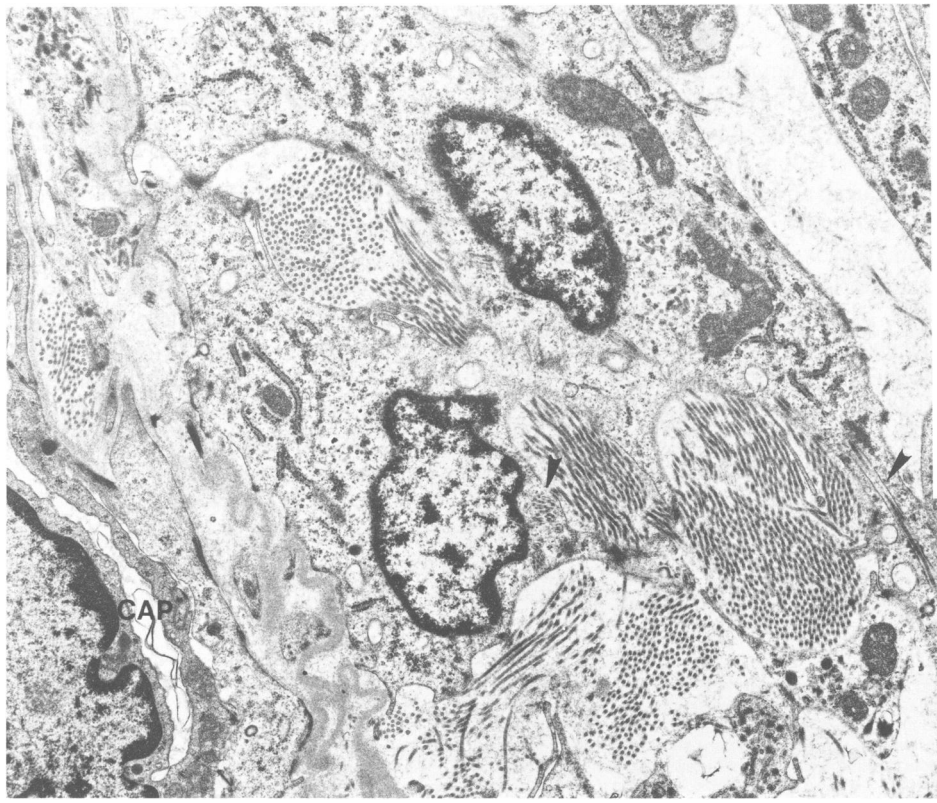
CAP
31

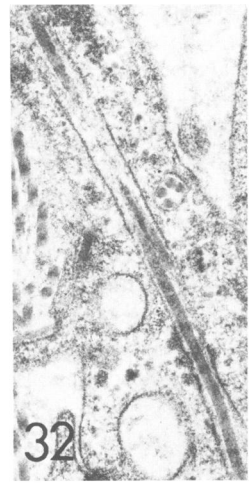
32

were also prominent. In later stages, the proliferative changes could be divided into two types, depending on whether or not intraalveolar fibrosis was present. Alveoli without intraalveolar fibrosis were lined by regenerating Type II alveolar epithelial cells, and the architecture of such alveoli eventually became more normal.

The intraalveolar migration of interstitial connective tissue cells, through gaps in the epithelial basement membranes, was one of the most important events responsible for the development of intraalveolar fibrosis. These changes occurred in alveoli in which regenerative changes in alveolar epithelial cells were less pronounced than was the case in alveoli without intraalveolar fibrosis. The cellular migration was followed by synthesis of extracellular components of connective tissue on the luminal side of the original basement membrane and by differentiation of intralveolar connective tissue cells into myofibroblasts and smooth-muscle cells. These changes are shown diagrammatically in Figure 41.

Changes in Alveolar Epithelial Cells

Proliferation of Type II epithelial cells is thought to be a nonspecific reaction to alveolar epithelial damage.[26,27] Such a proliferation of Type II cells was previously observed in early stages of paraquat toxicity.[9,22,25] The proliferating Type II cells observed in the present study typically protruded into the alveolar lumens. They had large nuclei, prominent nucleoli, conspicuous free ribosomes in their cytoplasm, few discontinuities of their basement membranes, and few contacts between their basal regions and subjacent interstitial cells. These changes are considered to be characteristic of rapidly proliferating Type II cells. In contrast to these cells, the Type II cells in normal lungs and in lungs of patients with chronic fibrotic lung disorders frequently have contacts with underlying connective-tissue cells.[5] These differences may be related to the severity of the damage and to the relative rates of proliferation. It has been suggested that Type II cells proliferate when alveolar epithelial-cell damage is only mild or moderate, and that when this damage is severe the Type II cells die and are replaced by epithelial cells of bronchiolar origin.[5]

Proliferating Type II cells are thought to be progenitors of Type I epithelial cells.[28-31] This concept is in accord with the observation that in later stages of paraquat toxicity, Type II cells were less numerous than in early stages, and Type I epithelial cells were predominant in less fibrotic regions. In the late stages, Type II epithelial cells protruded into alveolar spaces to a lesser extent than in previous stages. They also had more numerous basal microfoldings, discontinuities in their basement membranes, and areas of contact with the underlying connective tissue cells. These changes were especially prominent in cells which formed glandlike structures in fibrotic lesions. Smith and Fletcher[32] have emphasized the importance of epithelial–mesenchymal interactions in organogenesis of developing lung. The reestablishment of epithelial–mesenchymal interactions in paraquat-induced fibrotic lesions seemed to correlate with recovery from the injury.

Hyperplasia of epithelial cells of bronchiolar origin[6-8,26] and squamous metaplasia were prominent in severely fibrotic areas that showed little or no regeneration of alveolar epithelial cells. Squamous metaplasia was conspicuous in alveolar ducts associated with obliterated alveoli and in alveoli in which Type II epithelial cell hyperplasia was poor or absent, as is often the case in patients with fibrotic lung disorders.[5] The squamous-cell metaplasia also tended to disappear in association with the recovery process. Thus, this study confirms previous observations showing that bronchiolar epithelial hyperplasia and squamous metaplasia are associated with obliteration of alveoli and with poor regeneration of alveolar epithelial cells.[5]

Structural Changes in Extracellular Elements of Connective Tissue

The structural changes found in collagen fibrils, elastic fibers, and epithelial basement membranes were associated with marked alveolitis; and it seems reasonable to believe that such changes were caused by proteolytic enzymes released by the inflammatory cells. Alveolitis is known to occur in paraquat intoxication,[20,22,23] and the effects of inflammatory cells such as macrophages and neutrophils have been considered important in the development of paraquat-induced pulmonary fibrosis.[26] The various proteolytic enzymes in macrophages and neutrophils are able to damage Type I, III, and IV collagen and elastin.[34,35]

Figure 29—Group III. The original wall of an alveolus, shown at the *left* and in the *center*, contains relatively large elastic fibers and many spiraling collagen fibrils. The latter are found exclusively in alveolar interstitium. The intraalveolar space, shown at the *right*, contains a smooth-muscle cell (*S*), a myofibroblast (*MF*), and thinner collagen fibrils; this space is separated from the original alveolar wall by a wavy basement membrane. (Kajikawa stain, × 15,000) **Figure 30**—High magnification of the spiraling collagen fibrils shown in Figure 29. Note the large diameters and irregular cross-sectional shapes of these fibrils. (Kajikawa stain, × 35,000) **Figure 31**—Group III. Fibroblastlike cell which has engulfed collagen fibrils (*arrowheads*) is found in intraalveolar space. Note the capillary (*CAP*) and pericytelike cell, which are separated from the intraalveolar area by basement membrane. (Kajikawa stain, × 11,000) **Figure 32**—High magnification of engulfed collagen fibrils in the fibroblastlike cell shown in Figure 31. (Kajikawa stain, × 31,000)

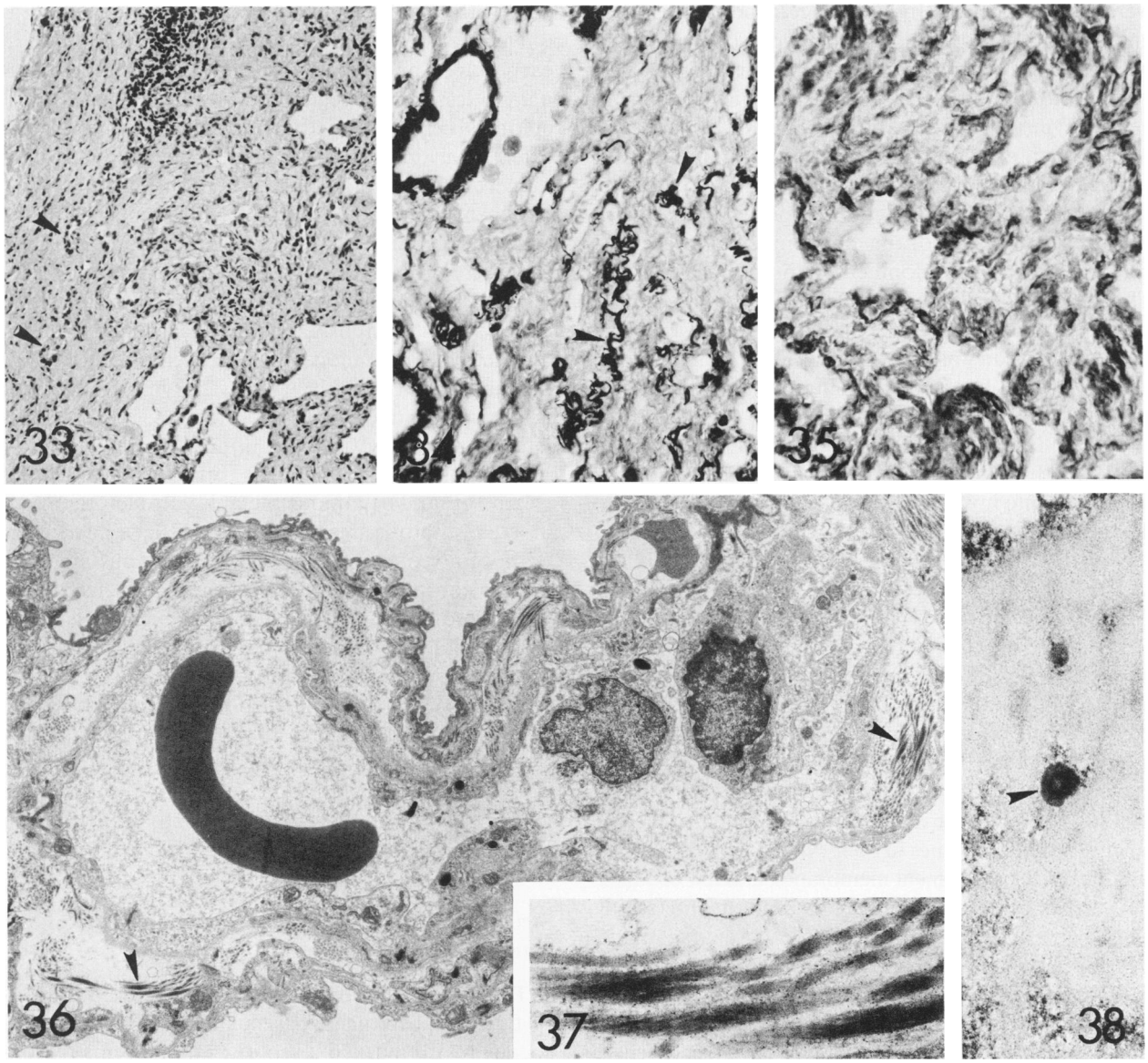

Figure 33—Eight weeks after paraquat administration (Group IV). Focal fibrotic lesion is associated with mild infiltration of lymphoid cells and with small glandlike structures (*arrowheads*). (H&E, ×110) **Figure 34**—Group IV. Elastic fibers (*arrowheads*) are embedded in dense fibrous tissue in areas of obliterated alveoli associated with intraalveolar fibrosis. (Hart's method, ×280) **Figure 35**—Group IV. Laminin is localized in the basement membranes of the alveolar walls and in areas which are embedded in fibrous connective tissue. (Immunoperoxidase, ×280) **Figure 36**—Group IV. Alveolar wall is lined mainly by Type I alveolar epithelial cells. No intraalveolar fibrosis is present. Spiraling collagen fibrils (*arrowheads*) are conspicuous in the interstitium. (Kajikawa stain, ×9600) **Figure 37**—High magnification of the spiraling collagen fibrils shown in Figure 36. (Kajikawa stain, ×70,000) **Figure 38**—Group IV. Amorphous components of elastic fiber are associated with small, electron-dense lamellar nodular masses (*arrowheads*). (×56,000)

Collagen Fibrils

In the early stages of paraquat toxicity, the collagen fibrils of alveolar septa appeared as thin, separated bundles. Later, twisted, frayed, spiraling collagen fibrils were found in some areas. Spiraling collagen fibrils have been described in certain heritable connective-tissue dysplasias, in which the skin is hyperextensible and fragile,[36] and also in numerous other conditions.[36] In the lung, these fibrils have been observed in pulmonary fibroleiomyoma,[37] pulmonary lymphangioleiomyomatosis,[38] experimentally induced pulmonary emphysema caused by exposure to NO_2,[39] human emphysema,[40] and idiopathic pulmonary fibrosis.[41] Two basic mechanisms can be responsible for the formation of spiraling collagen fibrils: 1) defective synthesis or aggregation of newly formed collagen and 2) dissociation, disaggregation or fraying of previously normal fibrils. The latter changes have been induced by treatment with urea or guanidine.[42] Similar breakdown of collagen fibrils has been induced by bacterial collagenase.[43]

We consider that partial dissociation or breakdown of collagen fibrils was responsible for the formation of the spiraling collagen fibrils found in the present study. Because newly formed collagen fibrils in intraalveolar spaces did not show these changes, it seems unlikely that the spiraling substructure resulted from a defect in collagen synthesis. It remains to be determined whether proteolytic enzymes from macrophages or neutrophils are capable of directly inducing a spiraling substructure in collagen fibrils.

Elastic Fibers

The elastic fibers in the lung of paraquat-treated animals appeared frayed and consisted of poorly outlined amorphous materials and many loosely arranged microfibrils; some microfibril bundles were dissociated from the amorphous materials. Similarly abnormal elastic fibers have been described in the early stages of experimental emphysema produced by intratracheal administration of elastase[44-46] and in human emphysema.[40] Emphysematous dilation of alveolar walls has been described in paraquat toxicity.[7,47] In the present study, the extent of damage of the elastic fibers generally correlated well with the degree of dilation of the alveolar spaces. In *in vitro* studies, similar fraying of elastic fibers resulted from brief incubation with elastase.[42,49] The frayed elastic fibers observed in the present study are presumed to be composed of loosely arranged amorphous materials, as suggested by a histochemical study of enzymatic digestion of elastin.[50]

In later stages of paraquat toxicity, small calcified nodular masses appeared between the amorphous components of elastic fibers. These calcified nodular masses probably are consequences of damage to elastic fibers. In addition, the calcified elastic fibers found in this study were associated with spiraling collagen fibrils. A similar association has been reported in pulmonary lymphangioleiomyomatosis,[38] human emphysema,[40] and other lung diseases, including idiopathic pulmonary fibrosis (Y. Fukuda, V. J. Ferrans, and R. G. Crystal, unpublished data). This association can be explained on the basis of damage caused by lysosomal enzymes of inflammatory cells on both the elastic fibers and the collagen fibrils.

Epithelial Basement Membranes

After epithelial cell denudation, epithelial basement membranes appeared uneven in thickness, frayed, and partially dissociated and disrupted. Similar but less severe changes were found in capillary basement membranes. Patchy breakdown[9] or focal absence[25] of the epithelial basement membranes in alveolar walls have been observed in paraquat intoxication but have not been described in detail. In the present study, immunohistochemical stains for Type IV collagen and laminin, which are important components of basement membranes,[51,52] demonstrated disruption of epithelial basement membranes in alveoli that had intraalveolar fibrosis. This disruption may be caused by hydrolytic enzymes released from inflammatory cells, because neutrophil elastase can damage Type IV collagen.[34] This enzyme also can digest the gingival epithelial basement membranes *in vitro*.[53]

Denuded basement membranes are thought to serve as a scaffolding for epithelial cell and endothelial cell regeneration.[54] It is likely that in areas where alveolar injury is mild, the gaps in the epithelial basement membranes remain small and become covered by regenerating epithelial cells; thus, if regeneration of epithelial cells is adequate, intraalveolar fibrosis will not develop. In contrast, if alveolar injury is severe, the gaps in the basement membranes are large, are not covered by growth of regenerating epithelial cells, and become the sites of penetration of connective-tissue cells into the alveolar luminal spaces. In some instances, the regenerating epithelial cells grow over a layer of fibrinous exudate deposited upon the luminal surface of the epithelial basement membrane, and for this reason they do not establish contact with a preexisting basement membrane. This leads to reduplication of the basement membrane, with the old basement membrane usually appearing wavy and convoluted.

Recruitment, Activation, and Migration of Connective-Tissue Cells

Intraalveolar fibrosis is one of the characteristic pathologic findings in paraquat intoxication.[8,10,12,23,25-27] In agreement with these previous findings, we observed activated fibroblasts in the areas of interstitial and intraalveolar fibrosis in paraquat pulmonary toxicity. These observations indicate that the intraalveolar fibrosis is mediated by fibroblasts which originate from the alveolar walls and migrate through the gaps of the epithelial basement membranes into alveolar lumina. A similar mechanism is of importance in the pathogenesis of the intraalveolar lesions that are frequently found in hypersensitivity pneumonitis.[55,56]

The fibroblasts migrating into the intraalveolar spaces had well-developed Golgi zones, which were located closer to the lumens than to the alveolar septal areas. The location of the Golgi zone has been thought to indicate the direction of movement of fibroblasts[51]; therefore, this observation supports the concept that these fibroblasts were migrating toward the alveolar lumens. Such fibroblasts became attached to the luminal sur-

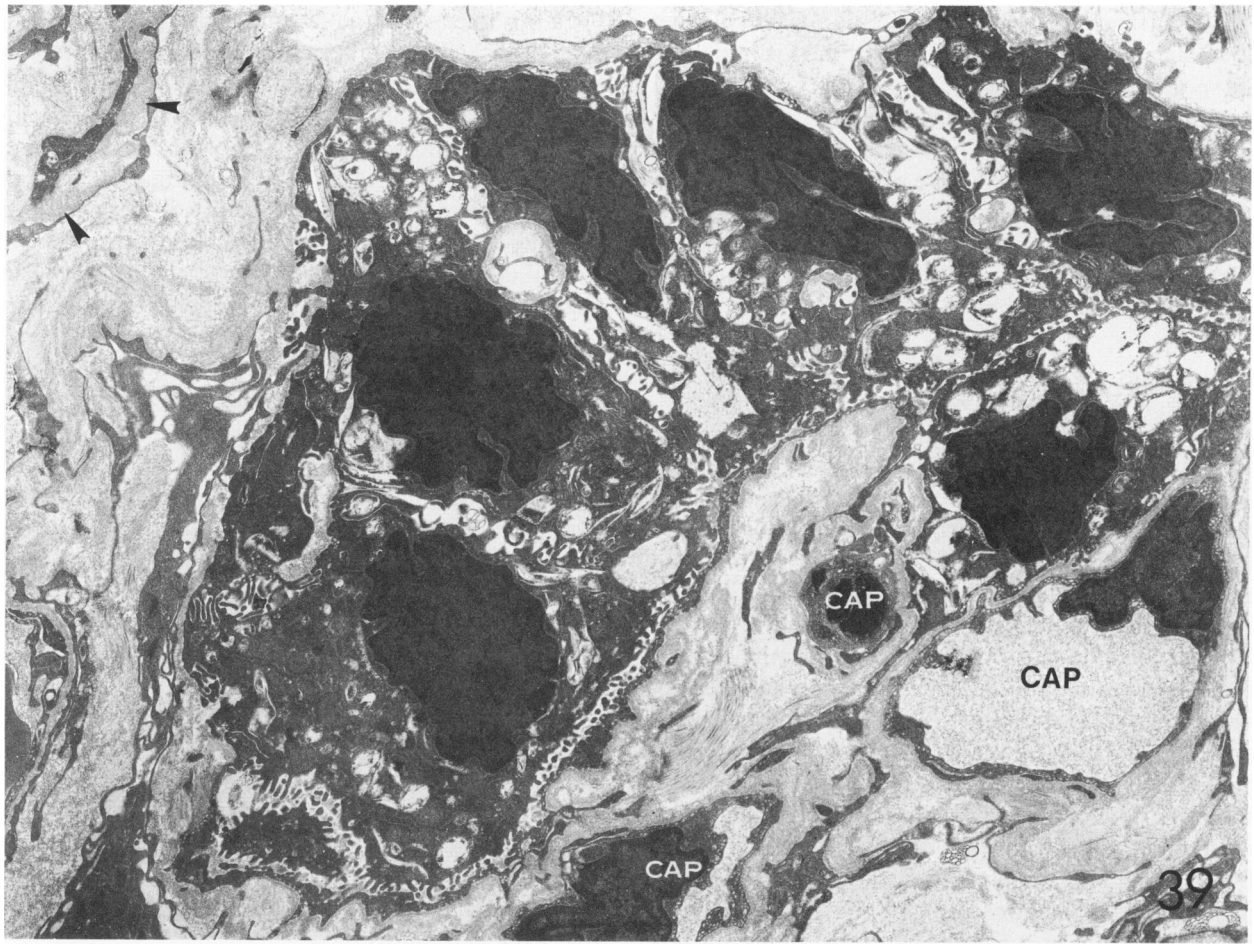
CAP
CAP
CAP
39

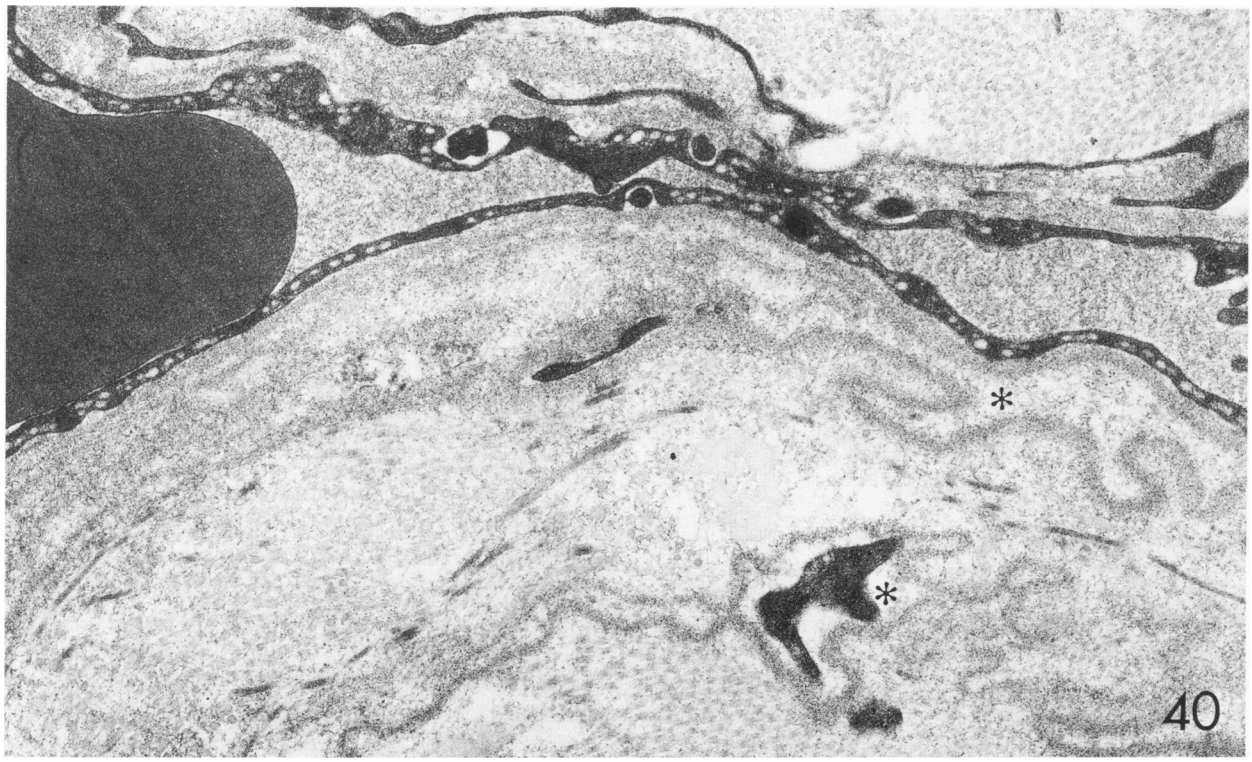
*
*
40

face of the epithelial basement membrane by means of cytoplasmic processes having dense plaques. Such plaques resembled the peripherally located cytoplasmic dense bodies that are normally present in the myofibroblastlike interstitial cells (Kapanci cells)[19] of alveolar septa at sites in which these cells come into close contact with the septal or abluminal surface of the alveolar epithelial basement membrane. These attachment plaques are not typical of ordinary fibroblasts but are in keeping with the tendency of these cells to differentiate into myofibroblasts and smooth-muscle cells similar to those normally present in alveolar septa. The markers of this differentiation are decreased amounts of rough-surfaced endoplasmic reticulum, increased numbers of actinlike filaments and peripherally located dense bodies, and newly formed basement membranes.[19] This differentiation can be regarded as part of an attempt to recreate the architecture of the alveolar septal wall, but on the "wrong" side of the basement membrane.

Bronchoalveolar lavage fluid from paraquat-exposed animals has been reported to contain increased amounts of fibronectin.[20] Alveolar macrophages from these animals produce increased amounts of fibronectin and spontaneously release a growth factor for fibroblasts. Normal alveolar macrophages exposed to paraquat *in vitro* can be induced to release this growth factor.[20] Fibronectin itself serves both as a chemoattractant and a growth factor for fibroblasts.[58] Thus, factors released from the macrophages in the alveolitis induced by paraquat probably are responsible for the recruitment and migration of the fibroblasts which mediate the development of pulmonary fibrosis.

Production of Connective-Tissue Components in Intraalveolar Spaces

The prominent extracellular components of connective tissue within alveolar spaces in paraquat-induced toxicity were collagen fibrils and elastic fibers. Proteoglycans were also prominent in the early stages but subsequently decreased in amount. The elastic fibers in intraalveolar spaces were fine and were easily detected by immunohistochemical methods and by electron microscopy.[59] In association with the appearance of elastic fibers, the connective tissue cells which had migrated into alveolar spaces became differentiated into myofibroblasts and smooth-muscle cells. A similar association between elastogenesis and differentiation of connective-tissue cells in the direction of smooth-muscle cells occurs in the primordia of alveolar septa in developing fetal lung.[60] The mechanisms controlling this type of differentiation remain unknown. As discussed above, the collagen fibrils within alveolar spaces were morphologically normal, in contrast to the spiraling collagen fibrils that were found exclusively in alveolar septa, and were considered to result from damage to preexisting fibrils. The alveolar walls also had increased numbers of normal collagen fibrils, which were presumed to be newly synthesized as part of the process of interstitial fibrosis. Immunohistochemical studies showed that the newly formed intraalveolar collagen was more intensely stained by antibody to Type I collagen than by antibody to Type III collagen. It is very difficult to judge the relative amounts of two different types of collagen on the basis of immunofluorescence observations; however, biochemical studies of pulmonary fibrosis in humans and experimental animals have demonstrated an increase in the ratio of Type I to Type III collagen.[61-63] Immunohistochemical studies of human fibrotic lungs also have shown a marked increase in Type I collagen and a marked reduction in Type III collagen in thickened septa.[64] These findings are consistent with the observation that cultured fetal lung fibroblasts synthesize much more Type I than Type III collagen.[65]

Remodeling of Alveolar Structures in Paraquat Lung

Intraalveolar fibrosis appears to be more important than interstitial fibrosis in mediating structural remodeling of the lung. Interstitial fibrosis, strictly limited to alveolar interstitium, will result only in thickening of alveolar septa. In contrast, intraalveolar fibrosis results in obliteration of alveoli and coalescence of alveolar walls, changes which correlate with loss of functional alveolar–capillary units. Several steps appear necessary for the remodeling of lung tissue in paraquat toxicity: 1) denudation and formation of gaps in the epithelial basement membranes; 2) a low rate, or absence, of al-

Figure 39—Group IV. A glandlike structure with a very narrow lumen is formed by alveolar epithelial cells within an area of fibrosis. The cells on one side of this structure are mainly Type I epithelial cells; those on the other side are Type II cells. Many cytoplasmic contacts are found between interstitial cells (*IN*) and the basal portions of Type II epithelial cells. The area at the lower right of the glandlike structure contains fibrous connective tissue and capillaries (*CAP*); this area probably represents a thickened alveolar septum. The area at the *upper left* of the glandlike structure probably represents a region of intraalveolar fibrosis (compare with the earlier stage of formation shown in Figure 16). Note the wavy original epithelial basement membrane (*arrowheads*), which is covered by the thin cytoplasm of interstitial cells (×6000) **Figure 40**—Group IV. A capillary is associated with denuded, thin, and discontinuous basement membranes and with dense fibrous tissue. Two areas (*asterisks*) which contain thin cytoplasmic processes and are demarcated by partially disrupted basement membranes probably correspond to previous lumens of alveoli that have collapsed. (Compare with Figure 25.) Collagen fibrils and elastic fibers now surround these areas completely. (×22,000)

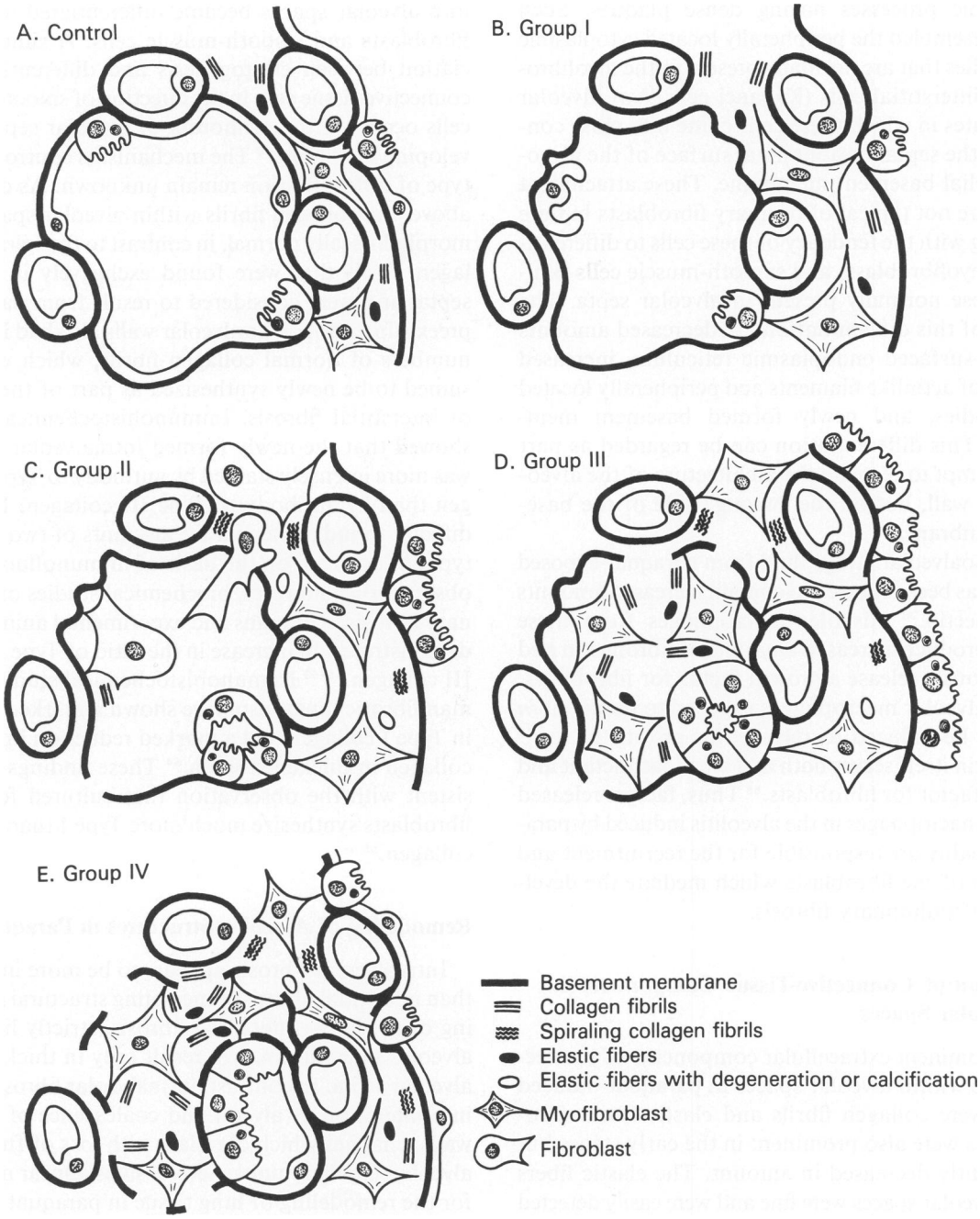

Figure 41—Diagram of structural remodeling of alveoli in paraquat toxicity. **A**—Control. Thin alveolar walls are lined by Type I and Type II epithelial cells. The basement membranes of the epithelial cells are fused with those of capillaries. Interstitial cells make contact with Type II epithelial cells through gaps in the epithelial basement membranes. **B**—Group I (2 or 3 days after paraquat administration). Many epithelial cells are detached and epithelial basement membranes are denuded in many areas. Interstitial edema results in focal dissociation of epithelial and endothelial basement membranes. **C**—Group II (1 week after paraquat administration). Some alveolar spaces having disrupted epithelial basement membranes are invaded by activated fibroblasts, which penetrate through the basement membranes. In these areas, some regenerated Type II epithelial cells form a glandlike structure. A few newly formed collagen fibrils are found in the intraalveolar space adjacent to fibroblasts. Spiraling collagen fibrils and frayed elastic fibers are conspicuous in the interstitium. **D**—Group III (3 or 4 weeks after paraquat administration). Some alveolar spaces contain myofibroblasts, smooth-muscle cells, bundles of normal collagen fibrils, and small elastic fibers. Epithelial basement membranes in these areas are more frayed and disrupted. Alveoli not showing intraalveolar fibrosis are (*right*) covered by increased numbers of Type II cells. Spiraling collagen fibrils and frayed elastic fibers are exclusively found in the interstitium of alveolar walls. **E**—Group IV (8 weeks after paraquat administration). Epithelial basement membranes in areas of intraalveolar fibrosis are more disrupted. Alveolar epithelial cells form glandlike structures embedded in fibrous tissue. Cells that are attached to the original epithelial basement membranes are mainly Type I cells; most of those in intraalveolar fibrotic lesions are Type II cells. Alveoli not showing intraalveolar fibrosis (*right*) are covered by Type I and Type II cells, and their structure is returning to normal.

veolar epithelial cell regeneration; 3) recruitment, activation, and migration of connective-tissue cells into alveolar lumens; 4) settlement of migrating connective-tissue cells with formation of cytoplasmic attachments to the luminal side of the epithelial basement membrane; 5) production of extracellular elements of connective tissue, so that the alveolar space is partially or completely incorporated into the interstitium and the apposed alveolar walls of the collapsed alveoli undergo fusion or coalescence; and 6) relining of the remaining portions of the alveolar space by epithelial cells, which often are of bronchiolar origin and show squamous metaplasia.

In this study, detailed evaluation of the topography of the denuded epithelial basement membranes was very helpful in understanding the process of structural remodeling. This evaluation was simplified by the fact that endothelial cells and their basement membranes showed very few alterations in the paraquat model, thus avoiding a major source of confusion in identification of the origin of the denuded basement membranes.

Remodeling associated with recovery from the injury was evident in the late stages of paraquat toxicity, as demonstrated by the following findings: 1) Some connective tissue cells in areas of intraalveolar fibrosis engulfed collagen fibrils, a change interpreted as indicative of lysis of collagen fibrils.[66-68] 2) Alveolar walls in areas not involved by intraalveolar fibrosis often showed nearly normal architecture. 3) In comparison with previous stages, the connective tissue components were decreased in amount and were compactly arranged; and myofibroblasts were decreased in size; however, the lesions of intraalveolar fibrosis associated with obliterated alveoli appeared to be irreversible.

The remodeling and inflammatory changes in the human fibrotic lung disorders, especially in idiopathic pulmonary fibrosis, are continuous or occur in repeated episodes, and for this reason they simultaneously show destructive and healing changes. Although morphologic changes in these disorders are more complex and more variable from one area to another than those observed in paraquat-treated lung, the concepts of pulmonary remodeling derived from this study may help in understanding the structural derangements in human fibrotic lung disorders.

References

1. Basset F, Lacronique J, Ferrans VJ, Fukuda Y, Crystal RG: Intraalveolar fibrosis: A second form of fibrosis of the interstitial lung disorders (Abstr). Am Rev Respir Dis 1984, 129 (Part II): A-72
2. Kuhn C, Askin FB, Katzenstein AA: Diagnostic light and electron microscopy, Diagnostic Techniques in Pulmonary Disease. Part I. Lung Biology in Health and Disease. Vol 16. Edited by MA Sackner. Marcel Dekker, Inc., 1980, pp 89-202
3. Katzenstein AA, Askin FB: Chronic interstitial pneumonia, interstitial fibrosis, and honeycomb lung, Major Problems in Pathology. Vol 13, Surgical Pathology of Nonneoplastic Lung Disease. Philadelphia, W. B. Saunders, 1982, pp 43-72
4. Spencer H: Pulmonary disease of uncertain etiology, Pathology of the Lung. Vol 2. Edited by H Spencer. Pergamon Press, 1977, pp 697-772
5. Kawanami O, Ferrans VJ, Crystal RG: Structure of alveolar epithelial cells in patients with fibrotic lung disorders. Lab Invest 1982, 46:39-53
6. Clark DG, McElligott TF, Hurst EW: The toxicity of paraquat. Br J Industr Med 1966, 23:126-132
7. Mattew H, Logan A, Woodruff MFA, Head B : Paraquat poisoning—Lung transplantation. Br Med J 1968, 28:759-763
8. Toner PG, Vetters JM, Spilg WGS, Harland WA: Fine structure of the lung lesions in a case of paraquat poisoning. J Pathol 1970, 102:182-185
9. Vijeyaratnam GS, Corrin B: Experimental paraquat poisoning: A histological and electron-optical study of the changes in the lung. J Pathol 1971, 103:123-129
10. Smith P, Heath D, Kay JM: The pathogenesis and structure of paraquat-induced pulmonary fibrosis in rats. J Pathol 1974, 114:57-67
11. Copland GM, Kolin A, Shulman HS: Fatal pulmonary intraalveolar fibrosis after paraquat injection. N Engl J Med 1974, 291:290-292
12. Borchard F: Ultrastrukturelle and lichtmikroskopische Befund bei drei protrahiert tödlich verlaufenen Paraquatvergiftungen. Pulmonologie 1974, 150:185-189
13. McDowell EM, Trump BF: Histologic fixatives suitable for diagnostic light and electron microscopy. Arch Pathol Lab Med 1976, 100:405-414
14. Rennard SI, Church RR, Rohrbach DE, Shupp S, Abe S, Heintt AT, Murray JG, Martin GR: Localization of the human fibronectin (Fn) gene on chromosome 8 by a specific enzyme immunoassay. Biochem Gen 1981, 19:551-556
15. Glanville RW, Kuhn K: Preparation of two basement membrane collagens from human placenta, Biochemistry of Normal and Pathological Connective Tissues. Paris, Centre National de la Recherche Scientifique, 1980, pp 65-68
16. Foidart JM, Berman JJ, Paglia L, Rennard SI, Abe S, Perantoni MS, Martin GR: Synthesis of fibronectin, laminin, and several collagens by a liver-derived epithelial line. Lab Invest 1980, 42:525-532
17. Graham RC, Karnovsky MJ: The early stages of absorption of injected horseradish peroxidase in the proximal tubules of mouse kidney: Ultrastructural cytochemistry by a new technique. J Histochem Cytochem 1966, 14:291-302
18. Kajikawa K, Yamaguchi T, Katsuda S, Miwa A: An improved electron stain for elastic fibers using tannic acid. J Electron Microsc (Tokyo) 1975, 24:287-289
19. Kapanci Y, Assimacopoulos A, Irle C, Zwahlen A, Gabbiani G: "Contractile interstitial cells" in pulmonary alveolar septa: A possible regulator of ventilation/perfusion ratio? Ultrastructural, immunofluorescence, and in vitro studies. J Cell Biol 1974, 60:375-392
20. Schoenberger CI, Rennard SI, Bitterman PB, Fukuda Y, Ferrans VJ, Crystal RG: Paraquat-induced pulmonary fibrosis: Role of the alveolitis in modulating the development of fibrosis. Am Rev Respir Dis 1984, 129:168-173
21. Murray RE, Gibson JE: A comparative study of paraquat intoxication in rats, guinea pigs, and monkeys. Exp Mol Pathol 1972, 17:317-325
22. Brooks RE: Ultrastructure of lung lesions produced by

ingested chemicals: I. Effect of the herbicide paraquat on mouse lung. Lab Invest 1971, 25:536–545
23. Smith P, Heath D: The pathology of the lung in paraquat poisoning. J Clin Pathol 1975, 28:81–93
24. Seidenfeld JJ, Wycoff D, Zavala DC, Richerson HB: Paraquat lung injury in rabbits. Br J Industr Med 1978, 35:245–257
25. Kelly DF, Morgan DG, Darke PGG, Gibbs C, Peason H, Weaver BMQ: Pathology of acute respiratory distress in the dog associated with paraquat poisoning. J Comp Pathol 1978, 88:275–294
26. Smith P, Heath D: Paraquat lung: a reappraisal. Thorax 1974, 29:643–653
27. Rebello G, Mason JK: Pulmonary histological appearances in fatal paraquat poisoning. Histopathology 1978, 2:53–66
28. Kapanci Y, Weibel ER, Kaplan HP, Robinson FR: Pathogenesis and reversibility of the pulmonary lesions of oxygen toxicity in monkeys: II. Ultrastructural and morphometric studies. Lab Invest 1969, 20:101–118
29. Bachofen M, Weibel ER: Basic pattern of tissue repair in human lungs following unspecific injury. Chest 1973, 65:14S–21S
30. Evans MJ, Cabral LJ, Stephens RJ, Freeman G: Renewal of alveolar epithelium in the rat following exposure to NO_2. Am J Pathol 1972, 70:175–198
31. Adamson IYR, Bowden DH: The type II cell as progenitor for alveolar epithelial regeneration: A cytodynamic study in mice after exposure to oxygen. Lab Invest 1974, 30:35–42
32. Smith BT, Fletcher WA: Pulmonary epithelial-mesenchymal interactions: Beyond organogenesis. Hum Pathol 1979, 10:248–250
33. Payan H, Monges G, Jouve MP, Saux MA, Pellegrin E, Garbe L: Intoxication par le paraquat. Étude ultrastructurale des lésions pulmonaires: A propos d'une observation. Arch Anat Cytol Pathol 1982, 30:33–38
34. Gadek JE, Hunninghake GW, Fell GA, Zimmerman RL, Keogh BA, Crystal RG: Evolution of the protease-antiprotease theory of human destructive lung disease. Bull Eur Physiopathol Respir 1980, 16:27–40
35. Crystal RG, Rennard SI: Pulmonary connective tissue and environmental lung disease. Chest 1981, 80S (suppl): 33S–38S
36. Ghadially FN: Extracellular matrix (extracellular components) Ultrastructural Pathology of the Cell and Matrix. 2nd edition. London, Butterworths, 1982, pp 881–947
37. Manabe T, Kikkawa Y: Helical structure of human native collagen. Arch Pathol Lab Med 1976, 100:259–264
38. Basset F, Soler P, Marsac J, Corrin B: Pulmonary lymphangiomyomatosis: Three new cases studied with electron microscopy. Cancer 1976, 38:2357–2366
39. Stephens RJ, Freeman G, Evans MJ, Calif MF: Ultrastructural changes in connective tissue in lungs of rats exposed to NO_2. Arch Intern Med 1971, 127:873–883
40. Belton JC, Crise N, McLaughlin RF, Tueller EE: Ultrastructural alterations in collagen associated with microscopic foci of human emphysema. Human Pathol 1977, 8:669–677
41. Crystal RG, Fulmer JD, Baum BJ, Bernardo J, Bradley KH, Bruel SD, Elson NA, Fells GA, Ferrans VJ, Gadek JE, Hunninghake GW, Kawanami O, Kelman JA, Line BR, McDonald JA, McLees BD, Roberts WC, Rosenbery DM, Tolstoshev P, Von Gal E, Weinberger SE: Cells, collagen and idiopathic pulmonary fibrosis. Lung 1978, 155:199–224
42. Lillie JH, MacCallum DK, Scaletta LJ, Occhino JC: Collagen structure: Evidence for a helical organization of the collagen fibril. J Ultrastruct Res 1977, 58:134–143
43. Kajakawa K, Nakanishi I, Yamamura T: The effect of collagenase on the formation of fibrous long spacing collagen aggregates. Lab Invest 1980, 43:410–417
44. Kuhn C, Yu S, Chraplyvy M, Linder HE, Senior RM: The induction of emphysema with elastase: II. Changes in connective tissue. Lab Invest 1976, 34:372–380
45. Miyazaki N, Takamoto M, Kinjo M, Ishibashi T: Ultrastructural studies of elastase-induced experimental emphysema. Jpn J Exp Med 1979, 49:241–150
46. Morris SM, Stone PJ, Snider GL, Albright JT, Franzblau D: Ultrastructural changes in hamster lung four hours to twenty-four days after exposure to elastase. Anat Rec 1981, 201:523–535
47. Greenberg DB, Reiser KM, Last JA: Correlation of biochemical and morphologic manifestations of acute pulmonary fibrosis in rats administered paraquat. Chest 1978, 74:421–415
48. Ross R, Bornstein P: The elastic fiber: 1. The separation and partial characterization of its macromolecular components. J Cell Biol 1969, 40:366–381
49. Braverman IM, Fonferko E: Studies in cutaneous aging: 1. The elastic fiber network. J Invest Dermatol 1982, 78:434–443
50. Fukuda Y, Ferrans VJ: The electron microscopic immunohistochemistry of elastase-treated aorta and nuchal ligament of fetal and postnatal sheep. J Histochem Cytochem 1984, 32:747–756
51. Martinez-Hernandez A, Miller EJ, Damjanov I, Gay S: Laminin-secreting yolk sac carcinoma of the rat. Biochemical and electron immunohistochemical studies. Lab Invest 1982, 47:247–257
52. Martinez-Hernandez A, Amenta PS: The basement membrane in pathology. Lab Invest 1983, 48:656–677
53. Cergneux M, Andersen E, Cimasoni G: In vitro breakdown of gingival tissue by elastase from human polymorphonuclear leukocytes. An electron microscopic study. J Periodont Res 1982, 17:169–182
54. Vracko R: Significance of basal lamina for regeneration of injured lung. Virchows Arch [Pathol Anat] 1972, 355:264–274
55. Basset F, Le Crom M, Decroix G: Etude ultrastructurale d'une biopsie pulmonaire au cours d'une maladie des élèveurs d'oiseaux: Pneumopathie interstitielle d'hypersensibilité. Presse Med 1970, 78:699–704
56. Kawanami O, Basset F, Barrios R, Lacronique JG, Ferrans VJ, Crystal, RG: Hypersensitivity pneumonitis in man: Light- and electron-microscopic studies of 18 lung biopsies. Am J Pathol 1983, 110:275–289
57. Trelstad RL: Mesenchymal cell polarity and morphogenesis of chick cartilage. Dev Biol 1977, 59:153–163
58. Bitterman PB, Rennard SI, Adelberg S, Crystal RG: Role of fibronectin as a growth factor for fibroblasts. J Cell Biol 1983, 97:1925–1932
59. Fukuda Y, Ferrans VJ, Crystal RG: Development of elastic fibers of nuchal ligament, aorta and lung of fetal and postnatal sheep: An ultrastructural and electron microscopic immunohistochemical study, Am J Anat 1984, 170: 597–629
60. Fukuda Y, Ferrans VJ, Crystal RG: The development of alveolar septa in fetal sheep lung: An ultrastructural and immunohistochemical study. Am J Anat 1983, 167: 405–439
61. Seyer JM, Hutcheson ET, Kang AH: Collagen polymorphism in idiopathic chronic pulmonary fibrosis. J Clin Invest 1976, 57:1498–1507
62. Reiser KM, Last JA: Pulmonary fibrosis in experimental acute respiratory disease. Am Rev Respir Dis 1981, 123:58–63
63. Haschek WM, Kelin-Szanto AJP, Last JA, Reiser KM, Witschi HP: Long-term morphological and biochemical features of experimentally induced lung fibrosis. Lab Invest 1982, 46:438–449
64. Madri JA, Furthmayr H: Collagen polymorphism in the lung: An immunochemical study of pulmonary fibrosis. Hum Pathol 1980, 11:353–366

65. Berg RA, Steinmann B, Rennard SI, Crystal RG: Ascorbate deficiency results in decreased collagen production: Under-hydroxylation of proline leads to increased intracellular degradation. Arch Biochem Biophys 1983, 226: 681–686
66. Rentería VG, Ferrans VJ: Intracellular collagen fibrils in cardiac valves of patients with the Hurler syndrome. Lab Invest 1976, 34:263–272
67. Gross J: An essay on biological degradation of collagen, Cell Biology and Extracellular Matrix. Edited by ED Hay. New York, Plenum Press, 1981, pp 217–258
68. Pérez-Tamayo R: Morphologic and biochemical aspects of collagen degradation, Collagen Degradation and Mammalian Collagenase. Edited by M Tsuchiya, R Pérez Tamayo, I Okasaki, K Murayama. International Congress Series, Excerpta Medica No. 601, 1982, pp 3–19

Acknowledgments

The authors wish to thank Dr. J Davidson and Dr. S. Shibahara for a gift of the anti-elastin antibody; Dr. H Kleinman for a gift of anti-laminin and anti-Type IV collagen antibody; Dr. R. Leapman for his assistance in X-ray microanalysis; Mrs. M. Yamaguchi for her assistance with transmission electron microscopy; Mrs. E. Wilhoite for photographic work; and Mrs. E. Beard for typing the manuscript.